Tracking developmental change in the dopamine system using neuromelanin-sensitive MRI in children and adults

Rami Al Haddad

A thesis submitted to the University of Ottawa in partial fulfillment of the requirements for the Doctorate in Philosophy degree in Cellular and Molecular Medicine

Department of Cellular and Molecular Medicine
Faculty of Medicine
University of Ottawa

Table of contents

Acknowledgements

I would like to express my deepest gratitude to my supervisor, Dr. Clifford Cassidy, for welcoming me into his lab and providing invaluable guidance and mentorship throughout my PhD journey. His expertise and dedicated support have been instrumental in shaping my development as a scientist. I am also very grateful to my co-supervisor, Dr. Synthia Guimond, for her insights and continual encouragement.

A sincere thank you to the members of my thesis advisory committee: Dr. Lauri Tuominen, Dr. Zachary Kaminsky, and Dr. Reggie Taylor. Their constructive criticism, thoughtful feedback, and unwavering support have been crucial in guiding my research. I would also like to extend my sincere thanks to Dr. Paul Albert for his invaluable input and contributions throughout this process.

I would also like to thank my colleagues in the lab, who have made this journey enjoyable. I am happy that I got to share my experiences with bright future scientists.

I am deeply grateful to my family in Lebanon for their constant belief in me, even from afar. Your support has been a steady source of strength.

To my beloved wife, Stephanie, your love, patience, and belief in me have been my greatest motivation. And to our princess, Liana, you are a beacon of hope and inspiration. I dedicate this work to both of you, knowing that your presence in my life has driven me to achieve my best.

Thank you to everyone who played a part in this journey, I could not have done it without you.

Abstract

The study of the dopaminergic system in humans has been predominantly obstructed by the lack of practical and advanced imaging techniques. Neuromelanin-sensitive MRI (NM-MRI) leverages the properties of NM, a byproduct of dopamine metabolism, to measure its accumulation in the Substantia Nigra (SN), and its impact on the function and integrity of the dopaminergic system, opening the potential for its use as a neuroimaging biomarker. In this thesis we explore NM-MRI to gain more insights into the function and dynamics of the dopaminergic system across the lifespan.

The first aim of this thesis is to identify the normative range of NM-MRI values in cognitively normal older individuals (53-86 years old), a key initial step towards its use as a clinical biomarker. Our results did not show any significant age-related change in NM metrics in this age range. The stable normative metrics in older individuals play an essential part in helping differentiate between normal aging processes and those marking the potential onset of neurodegenerative conditions.

The second aim explores the change in NM dynamics across the lifespan in the human brain. Two types of NM-MRI sequences are used to study these dynamics, Magnetization Transfer (MT) and Turbo Spin Echo (TSE). We found that throughout the SN, different clusters of voxels behave differently with age, highlighting the importance of voxelwise analysis when interpreting the patterns of NM accumulation within the SN, in parallel with looking at the SN as a whole structure.

The third aim looks for a potential correlation between NM signal within the SN and cognitive performance in young individuals. Our results show a strong positive link between NM signal accumulation in the SN and working memory performance, specifically localized in specific subregions of the SN. These results highlight the dynamic nature of the dopaminergic system in early life.

The fourth and last aim of this thesis compares the NM-MRI signal in a group of children and adolescents with Attention-Deficit-Hyperactivity-Disorder (ADHD) to age-matched healthy controls. A significant decrease in NM-MRI signal was observed in ADHD patients compared to their healthy peers, suggesting that lower dopamine levels in the SN could have an underlying role in the disorder. This makes NM a promising biomarker for diagnosis and treatment monitoring in ADHD.

Overall, this work reveals valuable insights into the differential development of NM patterns during life, reaffirming the growing utility of NM-MRI for future research and its clinical role for early identification of neurodegenerative and neurodevelopmental disorders.

Abbreviations

AADC - Aromatic L-Amino Acid Decarboxylase

ADHD - Attention-Deficit Hyperactivity Disorder

CBCL - Child Behaviour Checklist

CBT - Cognitive Behavioral Therapy

CDR - Clinical Dementia Rating

CHEO - Children's Hospital of Eastern Ontario

CNR - Contrast-to-Noise Ratio

COMT - Catechol-O-Methyltransferase

CUAD - Chemical Use Abuse and Dependence Scale

DNA - Deoxyribonucleic Acid

DSM-5 - Diagnostic and Statistical Manual of Mental Disorders-5

FDA - Food and Drug Administration

FHAM - Family History Assessment Measure

FoV - Field of View

HPLC - High-Performance Liquid Chromatography

ICC - Intraclass Correlation Coefficient

L-DOPA - L-3,4-dihydroxyphenylalanine

LSWM - List Sorting Working Memory

MACE - Maltreatment and Abuse Chronology of Exposure

MBI-C - Mild Behavioural Impairment Checklist

MMSE - Mini-Mental State Examination

MNI - Montreal Neurological Institute

MAO - Monoamine Oxidase

MRI - Magnetic Resonance Imaging

MT - Magnetization Transfer

NIH - National Institutes of Health

NM - Neuromelanin

NM-101 - Neuromelanin-MRI software version 1.0.3 by Terran Biosciences

NM-MRI - Neuromelanin-Sensitive MRI

NPI - Nominated Principal Investigator

PD - Parkinson's Disease

PET - Positron Emission Tomography

PDMS - Pubertal Development Scale and Menstrual Cycle Survey

PQ-B - Prodromal Questionnaire Brief

PQ-BC - Prodromal Questionnaire Brief-Child Version

REDcap - Research Electronic Data Capture

ROI - Region of Interest

ROS - Reactive Oxygen Species

SAIQ - Sports and Activities Involvement Questionnaire

SCID - Structured Clinical Interview for DSM

SMEQ - Social Media Engagement Questionnaire

SN - Substantia Nigra

SNpc - SN pars compacta

SNpr - SN part reticulata

SPECT - Single-Photon Emission Computed Tomography

STQ - Screen Time Questionnaire

TE - Echo Time

TH – Tyrosine Hydroxylase

TR - Repetition Time

TRIAD - Translational Biomarkers in Aging and Dementia

TSE - Turbo Spin Echo

VMAT - Vesicular Monoamine Transporter

VTA - Ventral Tegmental Area

List of figures

List of tables

Chapter 1: Introduction

1.1 The Dopaminergic system

Dopamine is a catecholamine that serves as a neurotransmitter in certain areas of the central nervous system (CNS).[1] Dopamine synthesis starts by the uptake of the amino acid, tyrosine, into the cytosol of the dopaminergic neurons (Figure 1).[2,3] Tyrosine then undergoes a hydroxylation reaction catalyzed by tyrosine hydroxylase to become L-DOPA (L-3,4-dihydroxyphenylalanine).[2,3] The hydroxylation part of tyrosine is known to be the rate-limiting step in the process, making it slow and well regulated.[2,3] The following step is the decarboxylation process.[4,5] It is a quick reaction that takes place inside the cytoplasm of the dopaminergic neurons localized in specific regions of the brain, such as the Substantia Nigra (SN) and the Ventral Tegmental Area (VTA).[4,5] Decarboxylation is catalyzed by an enzyme called DOPA decarboxylase, also known as the aromatic L-amino acid enzyme decarboxylase (AADC).[5] The carboxyl group is removed from L-DOPA, and hence dopamine is formed.[2,6]

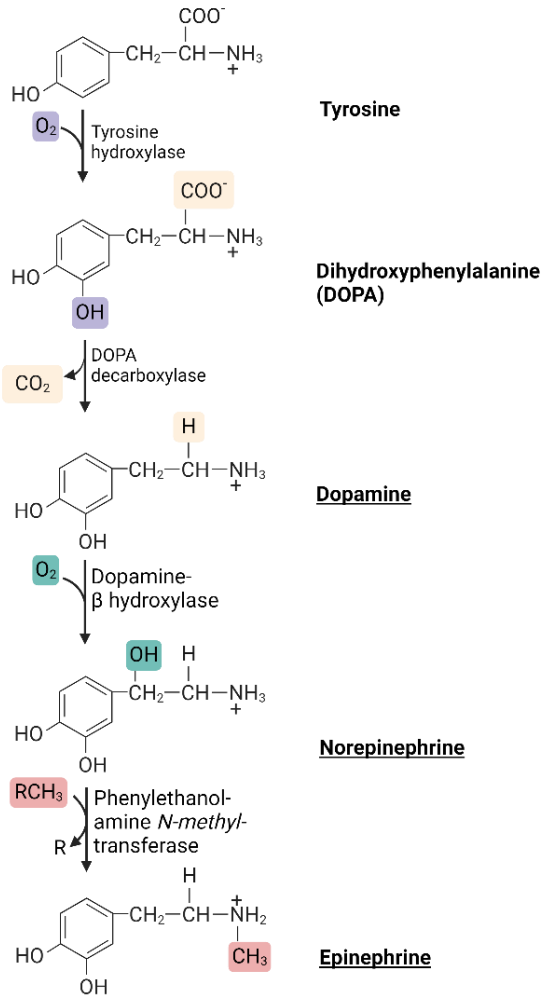

Figure 1. Dopamine synthesis pathway. *Tyrosine is hydroxylated by tyrosine hydroxylase (TH) to form L-DOPA. L-DOPA is then decarboxylated by AADC to produce dopamine.*[2] Created with BioRender.com

Newly synthesized dopamine is then transferred into the synaptic vesicles of the neurons through a proton gradient uptake process operated by the vesicular monoamine transporter (VMAT) (Figure 2).[7] Dopamine is stored there to avoid its degradation and oxidation by other cytoplasmic enzymes such as monoamine oxidase (MAO) and catechol-O-methyltransferase (COMT), until a neuronal signal triggers its release.[7,8]

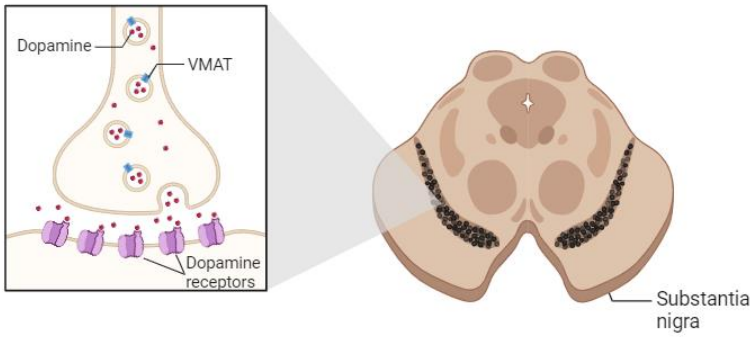

Figure 2. Dopamine release from dopaminergic neurons. *Dopamine is released after an action potential triggers the opening of voltage-gated calcium channels, causing synaptic vesicles containing dopamine to fuse with the presynaptic membrane, releasing dopamine into the synaptic cleft.* [9,10] Created with BioRender.com

Several steps are involved in the synthesis process of dopamine, and they all have a crucial role in maintaining the appropriate levels of dopamine in the brain for a healthy physiological function.[2,4,9] The synthesis is also accompanied by a feedback loop mechanism that helps avoid neuronal damage and neurotoxicity by preventing excessive deposit of dopamine in the brain.[1,9,11] Dopaminergic neurons are abundant in multiple but specific brain regions, such as the hypothalamus, SN and VTA.[12] These key regions are known to control motor skills, reward processing, mood regulation, cognition and endocrine control.[1,12]

One region of interest is the SN; It is small nuclei in the midbrain that has an important role in dopamine synthesis, storage and release.[13] The SN is divided into two regions: the SN pars compacta (SNpc), which is mainly composed of dopaminergic neurons that project to the striatum and form the nigrostriatal pathway.[13] This pathway plays a role in motor skills, as well as cognitive functions that include memory formation.[14] The second region is the SN pars reticulata (SNpr), which contains GABAergic neurons that have an inhibitory role once they fire their signals to the thalamus and other brain areas.[13]

Many neurological disorders and physiological dysfunctions are associated with malfunction in the dopaminergic neurons in the brain.[1,14,15] Having a deep and proper understanding of their function, including the formation, release, storage of dopamine, the different signaling pathways they trigger, and

which key brain regions are involved, helps understand, diagnose and eventually develop appropriate treatments and therapies for neurological and psychiatric disorders.[1,15,16]

1.2 Dopamine receptors and the nigrostriatal pathway

Dopamine can initiate signaling pathways that excite neurons and induce synaptic plasticity by binding to its appropriate receptors.[14,16] Dopamine receptors are G-protein coupled receptors categorized into two groups: the D1-like group, which includes D1 and D5 receptors, while D2, D3 and D4 receptors are part of the D2-like group.[16] Upon binding to D1-like receptors, stimulatory G proteins are activated, triggering a cascade of events that lead to the phosphorylation of target proteins that influence neuronal excitability.[17] On the other hand, the inhibitory G proteins are activated in D2-like receptors, reducing neuronal excitability.[17] Dopamine receptors are condensed in the striatum, as well as the prefrontal cortex and limbic system, where they control emotions, motor skills and cognitive behaviour.[16,18–20] They also

control the activation of several signaling pathways such as the mesolimbic, mesocortical and nigrostriatal pathways (Figure 3).[16,19,20]

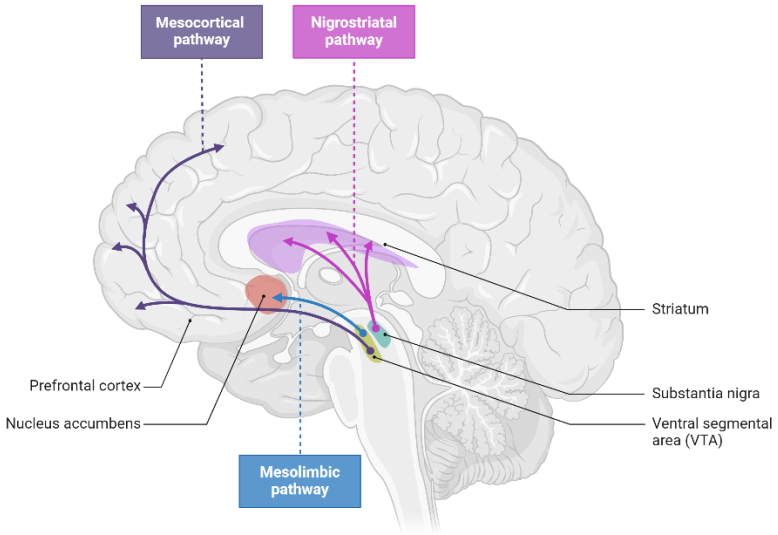

Figure 3. Nigrostriatal, mesolimbic and mesocortical pathways in the human brain. *This figure illustrates the major dopaminergic pathways in the human brain.* [18] Created with BioRender.com

1.2.1 The nigrostriatal pathway

The nigrostriatal pathway originates from the SN and extends its dopaminergic neurons mainly to the dorsal striatum of the basal ganglia, but some also reach the ventral striatum.[21] The dorsal striatum is known to be involved in motor and cognitive functions, while the ventral striatum is mostly associated with limbic functions such as reward and motivation.[21] Therefore, the nigrostriatal pathway plays an important role in planning and executing voluntary movements, cognitive skills such as attention, working memory, and emotions.[20–23] The SN is a heterogenous structure in the brain that is subdivided into different parts, and each part is involved in either the motor skill, cognition or emotional regulation.[24,25] Having a better understanding of the involvement and function of each subregion in the SN can help address the different neurological disorders associated with disruptions in the nigrostriatal pathway affecting movement, cognition and emotions.[25]

1.2.1.1 The nigrostriatal pathway and motor control

The nigrostriatal pathway is fundamental for motor control, specifically for the planning and execution of voluntary movements.[20,26] Movement is mainly controlled by the crosstalk between the excitatory direct pathway and the inhibitory indirect pathway that take place in the basal ganglia.[27–29] A recent study showed that Parkinson's Disease (PD) has been associated with the degeneration of the dopaminergic neurons in the SNpc, causing tremor, rigidity and bradykinesia, the most notorious symptoms of this disorder.[26,30–32] This indicates that the dopaminergic neurons in the SNpc are the ones responsible for releasing dopamine to coordinate voluntary movements.[26,31] Motor control starts with the excitatory direct pathway, when dopamine binds to D1 receptors on the striatal neurons, inducing movement.[19,29,31,33] This is followed by the inhibitory indirect pathway, where dopamine binds to D2 receptors, and suppresses unwanted movements.[26,29] The crosstalk between the indirect and direct pathways is what coordinates the movements properly.[29,32] Any disruption in this balance is believed to be a major contributor to any motor impairment and dysfunction, such as the case of PD.[19,26,29,34] The loss of dopaminergic input in PD leads to decreased activity in the direct pathway and increased activity in the indirect pathway, further contributing to PD's motor symptoms.[19,26,28]

1.2.1.2 Cognitive processes: working memory and attention

Working memory and attention are two additional functions that are tightly controlled by the nigrostriatal pathway.[26,35]

Working memory is the process by which information is stored for a short period of time and manipulated to achieve complex cognitive tasks such as learning, reasoning and comprehension.[35] This process is supported by dopamine signaling in the striatum and the cortex, although our main focus for this thesis will be on the nigrostriatal pathway.[27,35] The role of the dopaminergic system in working memory has been elucidated by numerous human imaging studies.[27,30] Some Positron Emission

Tomography (PET) studies have shown that working memory performance is closely correlated with dopamine release in the striatum.[27,35] One PET study showed that reduced dopamine release in key brain regions, including the associative striatum, is associated with poorer performance in working memory tasks.[27,30] In addition to PET studies, functional MRI (fMRI) studies have also been used to test the involvement of the nigrostriatal pathway in working memory.[30,36] Striatal activation is the main outcome during working memory tasks, with increased activation as the cognitive load increases.[27,30] This demonstrates the role of dopamine on cognition, implicating brain regions beyond the prefrontal cortex, and involving striatal circuits.[24,27,30]

Additional information into how dopamine influences working memory comes from animal studies.[37–40] Research on non-human primates has shown that disrupting dopamine transmission by blocking receptors caused major impairments in working memory tasks, highlighting the importance of dopaminergic signaling in cognitive function.[37,38] Goldman-Rakic's studies contributed to demonstrating how the nigrostriatal pathway modulates cognitive function.[39,40] Through the use of 6-hydroxydopamine and D1 receptor blockade in the prefrontal cortex, it was found that both excessive and insufficient dopamine levels could impair cognitive function, demonstrating the importance of a balanced dopaminergic system.[37,39,40] This research group also illustrated, through pharmacological manipulation of dopamine levels in non-human primates, that the nigrostriatal pathway is a key contributor to working memory, and established a foundation for understanding the neurobiological mechanisms underlying cognitive processes in primates.[37–40]

In addition to human primates, rodent models played an essential role in studying the role of dopamine in working memory.[41] Disruptions in the nigrostriatal pathway, either through lesions or pharmacological manipulations has been shown to impair working memory.[42] One rodent study showed the critical role of the nigrostriatal pathway in regulating specific cognitive processes; this group used a mouse model known as Pitx3-deficient aphakia mice, that exhibits a loss of dopaminergic neurons in the

SN.[43] These mice showed significant impairments in tasks related to working memory such as T-maze, and rotarod learning, while their performance is tasks like social transmission of food preference remained unaffected.[43] Research on rodents also shows how essential D1 and D2 receptors are in maintaining cognitive abilities.[44] For example, a more recent study highlighted the importance of dopamine signaling using DAT, by disrupting the insertion of dopamine D1 receptors into the cell membrane of rat models. These rats showed significant impairments in social interactions but maintained their usual motor capabilities.[45]

The role of the nigrostriatal pathway in working memory is supported by numerous studies done in humans and animals.[27,30,31,37–39,44,46] The striatum plays a major role, where dopamine signaling modulated by cortical inputs is what maintains and helps manipulate information in tasks involving working memory.[27,39,44] These findings contribute as evidence to move forward in investigating the NM signal in the SN and performance on dopamine-related cognitive tasks, making them particularly relevant to this thesis. Exploring this relationship could bring great understanding of the role of the dopaminergic system in cognitive function.

1.2.1.3 Dopamine's role in attention

Another cognitive ability regulated by the nigrostriatal pathway is attention, which consists on the ability to concentrate on a task and maintain focus for a prolonged period of time.[47,48] Dopamine signaling plays a role in guiding attention towards the stimuli that are important or rewarding, thus improving cognitive performance and higher success in achieving specific objectives or desired outcomes.[47–49] Any changes in the dopaminergic signaling in the striatum can cause a disruption in attention, affecting daily tasks and the ability to shift attention from one stimulus to another, emphasizing again the crucial role of dopamine and the nigrostriatal pathway in regulating cognitive skills.[48,49]

1.2.1.4 Attentional deficits and neurological disorders

Several psychiatric disorders, including Attention-Deficit-Hyperactivity-Disorder (ADHD), are associated with a disruption in the nigrostriatal pathway.[50] This disorder manifests by impulsivity, lack of focus and inability to complete a full task without getting distracted.[51] These symptoms are potentially due in part from abnormalities in dopamine transmission in the striatum, leading to attentional deficits and potential other neurological disorders.[50,51]

1.2.1.5 Emotional regulation and reward processing

In addition to cognitive skills, emotional regulation and reward processing are also modulated by the nigrostriatal pathway.[52,53] Dopamine plays a role in promoting motivational feelings, as well as directing people towards the striking and remarkable experiences, allowing individuals to learn from both positive and negative outcomes.[52,54] It can act as a "prediction error signal" within the striatum, where the dopaminergic neurons not only respond to the rewarding stimulus but also to the cues leading to that reward, which in turn help reinforce positive behavior and learning.[55,56] The prediction error is the difference between what is expected and what ends up actually happening.[57] An outcome that exceeds expectations is a positive prediction error, and this leads to the reinforcement of the behaviour that led to the outcome.[57] A negative prediction error is when the outcome is worse than expected, leading to adjustments in behaviour triggered by the desire to avoid disappointment in the future.[57] Prediction error serves as a sign for critical learning and adjustments of behaviours, processes regulated by dopamine activity.[57]

1.3 Historical and scientific advancements in dopamine research

One of the first groundbreaking projects identifying dopamine as neurotransmitter dates back to the 1950s and was accomplished by Arvid Carlsson and colleagues.[58] Dopamine discovery constituted the foundation that all subsequent research into the dopamine system was based on, and greatly helped our understanding of the role of dopamine in brain function and pathology.[58,59] Carlsson's team initially established the critical role that dopamine plays in movement and motor function.[59] This was the first step in demonstrating the magnitude of dopamine's involvement in the CNS.[59] Subsequently, the groundwork of the dopamine hypothesis of schizophrenia was established, suggesting that one of the fundamental signs of this disorder is abnormal dopamine activity.[58,60,61] Shortly after the discovery of dopamine and its identification as a neurotransmitter, another group led by Oleh Hornykiewicz found that individuals with PD show significant loss of dopamine.[62] This finding, in addition to the dopamine role in movement discovered by Carlsson and colleagues reinforced the notion of a connection between low dopamine levels and motor impairments.[58,60] It therefore facilitated future advancements for dopamine replacement therapies, including L-DOPA, which still serves as an essential part of PD treatment.[34,63]

The dopamine hypothesis of schizophrenia, proposed in the 1960s, remains one of the hypotheses that changed our understanding of psychiatric disorders.[60] It suggests that the main reason behind schizophrenia's positive symptoms can be abnormal changes in dopamine transmission in certain brain areas.[60] This hypothesis shed light on the importance of the nigrostriatal pathway in the development of positive symptoms, including delusions and hallucinations.[60,64] Recent studies confirm the dopamine hypothesis of schizophrenia by demonstrating that most antipsychotic drugs effective in the treatment of patients with schizophrenia block dopamine D2 receptors.[16,22,65] Moreover, neuroimaging studies looking at the human brain such as PET and single-photon emission computed tomography (SPECT), further supported this hypothesis by showing dysregulated dopamine function in patients with schizophrenia.[66–

[68] In addition to PD and schizophrenia, alterations in dopamine levels are considered to be underlying causes in conditions such as multiple system atrophy and supranuclear palsy.[68,69] Dopaminergic dysfunctions are involved in a large number of neurodegenerative disorders and the therapeutic interventions of dopamine research are extensive.[66,70]

1.4 Developmental trajectory of the dopamine system

Beginning in early fetal life, and extending well into adulthood, the development of the dopaminergic system is a complex and dynamic process.[71] The proper functioning of motor, cognitive, and emotional habits depends on the development of the dopaminergic system (Figure 4).[72,73]

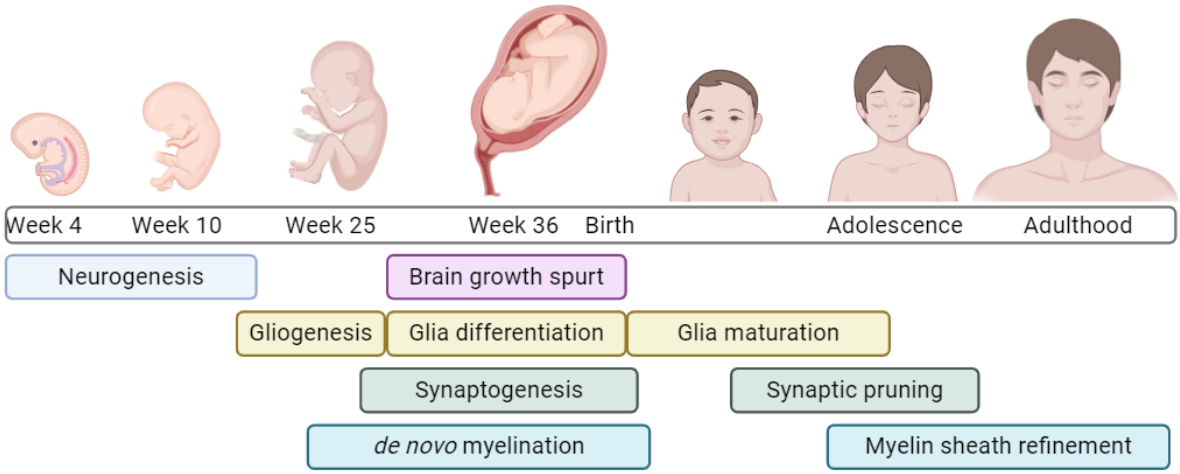

Figure 4. Timeline highlighting peak neurodevelopmental processes in humans.[73] Created with BioRender.com

1.4.1 Embryogenesis and early development

Early in embryogenesis, neural progenitor cells proliferate and differentiate, before establishing connections with their target regions, including the prefrontal cortex, striatum, and limbic structures.[74] In parallel, dopaminergic neurons emerge from the midbrain and migrate to critical dopaminergic structures including the VTA and the SN.[75,76] These actions are essential for the subsequent development of dopaminergic pathways that will eventually regulate several indispensable psychological functions.[14] The postnatal period is distinguished by rapid brain development, where extensive remodelling takes place to strengthen and refine the dopaminergic system's neural circuits.[77] This is accompanied by significant dendritic and axonal growth and carries over to early childhood phases.[78,79]

1.4.2 Adolescence: From axon guidance and targeting to synaptic pruning and myelination

During adolescence, changes shaping the adult brain function and behaviour develop.[80] During this period, unique and critical neurodevelopmental processes help shape the dopaminergic system. Axon guidance and targeting help form essential connections supporting cognitive and behavioural functions, while synaptic pruning and increased myelination facilitate neural circuit refinement, including circuits that underlie dopamine function.[81]

Axon guidance and targeting are processes guided by Netrin-1 receptor.[79,82,83] the Netrin-1/DCC cue system acts as a guidance cue and plays an essential role in axon targeting and synapse formation. By mediating axons' navigation and target interactions, it directs dopamine axons to the prefrontal cortex, a process that establishes axon connections in the right regions.[82,83] When the Netrin-1/DCC guidance pathway is disrupted, axons can be misdirected, leading to changes in connectivity that can be a reason behind susceptibility to psychiatric disorders.[83] Studies show that exposure to some recreational drugs during adolescence in mice can up-regulate Netrin-1 and/or DCC expression, rerouting axons, and missing connections, highlighting the vulnerability of this developmental period.[84] One study showed that amphetamine exposure downregulates the expression of DCC during early and mid adolescence through different mechanisms. This study underscores the importance of the Netrin-1/DCC cue system during this neurodevelopmental phase.[84]

The elimination of excess neurons and synaptic connections that highlights CNS changes during adolescence is known as synaptic pruning.[85] This process removes repetitive or weak neural connections that were created during early development, pre and postnatally, thereby tuning different neural pathways, including dopaminergic pathways.[74,85] Synaptic pruning is the major contributor to creating more defined and efficient neural circuits.[52,85,86] In a recent study using recurrent neural networks, the

effects of synaptic pruning on working memory and reinforcement learning were explored.[87] The results showed that pruned networks performed better in these tasks compared insufficiently or unpruned networks.[87] Moreover, study on rodents showed that disrupted synaptic pruning in adolescent mice achieved by downregulating a subclass of GABA receptors lead to an increase in amygdala activation, causing increased anxiety in late adolescence to early adulthood, contributing to the onset of several neuropsychiatric disoders.[88] This study highlights the role of synaptic running and increased risk of mental disorders, like depression and anxiety.[88]

Increased myelination is also an essential process marking the adolescence period.[89] Myelination is known to amplify efficiency and connectivity, fundamental to cognitive and emotional maturation in adolescence, by wrapping axons with an insulated myelin sheath.[90,91] In dopaminergic pathways, this process plays a crucial part in the development of higher cognitive functions by speeding up communication between different brain regions.[78,92,93] A recent imaging study used macromolecular protein fraction, a new quantitative MRI technique to measure myelin density in 9-17 year old adolescents.[94] This group found that increased cortical gray matter myelination, mainly in the parietal lobe, was highly correlated with memory and language skills, underscoring the role of myelination in behavioural and cognitive development during adolescence.[94]

Substance use during adolescence impacts attention, executive functions, and memory, due to its effects on specific brain regions like the prefrontal cortex and hippocampus.[95] Studies showed that adolescents with a history of heavy drinking demonstrated functional differences in their prefrontal cortex and hippocampus compared to healthy controls.[96] In addition, their performance in learning and working memory tasks was poorer than their nondrinking peers.[96] Earlier use has also been correlated with higher risks of psychopathologies, including depression, anxiety, and schizophrenia.[95–97] Another study showed that all types of substance use disorders were highly prevalent in a patient group with difference psychiatric disorders, such as bipolar disorder and schizophrenia, with alcohol consumption being the

most prevalent in every psychiatric category.[98] Substance use during this phase can also cause disruptions in the reward system, increasing vulnerability to future substance use disorders.[98,99]

The crucial role that the adolescence period plays in healthy brain development makes it a window of vulnerability for the onset and development of neuropsychiatric disorders including ADHD, psychosis, and substance use disorders.[93,100] For example, changes in receptor and transporter density and/or availability during this period of life can cause major behavioural deficits, especially when excitatory and inhibitory dopaminergic pathways are affected; this is what contributes to the most common symptoms of ADHD.[93] Thus, understanding the developmental trajectory of the dopaminergic system during adolescence is central to the search for early windows of intervention that can reduce the impact of dopamine-related disorders.

Reward pathways are particularly dynamic and heavily influenced by dopamine during this period.[101] This heightened sensitivity may cause the development of substance use disorders during adolescence, mainly due to the increased tendency towards risk-taking behaviours, making adolescents more vulnerable to activities like alcohol consumption, drug use, and other reward-seeking behaviours.[93] The reasons behind this increased sensitivity are still not very clear, but research suggests that it may be due, in part, to some tuning of the dopaminergic system that makes some individuals more vulnerable to seek out high-risk behaviour linked with higher rewards.[102]

Changes that occur during adolescence play a crucial role in emotional and cognitive development, through axon guidance and targeting, synaptic pruning and myelination.[1,93] The sensitivity of these processes increases the risk of the onset of dopamine-related disorders if any dysfunction affects them.[1,93] This marks adolescence as a key period in the maturation of the dopaminergic system.[78]

1.4.3 Adulthood: stability and plasticity

In adulthood, the dopaminergic system becomes relatively stable, though some plasticity is retained for learning and behavioural flexibility, allowing the brain to respond to new challenges and changes in the surrounding environment.[103,104]

As the brain ages, one of the most pronounced neurobiological changes is a degradation of dopaminergic function.[103] This can contribute to the cognitive and motor deficits that are characteristic of ageing.[26,103] A number of mechanisms can contribute to these declines, including reduced dopamine synthesis, limiting its levels for neural communication.[9,103] Reduced sensitivity to dopamine receptors and loss of dopaminergic neurons, particularly in the SN, can be considered as additional mechanisms contributing for age-related cognitive decline.[26,103,104] Cognitive deficits seen more often late in adulthood are partly due to the changes in the dopaminergic system.[26,105] Impairment in executive functions, such as problem-solving, planning and multitasking, are particularly common with age.[26,105] Working memory and processing speed, the time it takes to perceive, understand, and respond to information, all decline with age.[26,105,106] These combined effects emphasise the wide-ranging influence of age-related changes of the dopaminergic system on neural function, which is operating across the brain.

In addition to the natural cognitive decline during late adulthood, some functional impairments tend to increase the risk of onset and progression of neurodegenerative diseases.[105–107] One of the most noticeable and common consequences of severe dopaminergic neuron loss in the SN is PD.[26,36,108] Other neurodegenerative disorders such as Lewy body dementia, are also characterized by impaired dopaminergic function leading to the cognitive and behavioural symptoms of the disorder.[107,109]

1.5 Clinical implications of understanding the dopaminergic system

Understanding the function and development of the dopaminergic system is increasingly becoming a research area of interest because of the immense effect of this system on neurodegenerative and psychiatric disorders. Similar to any disorder, early detection and intervention in cases of abnormal development of the dopaminergic system can potentially improve outcomes for individuals with neurodevelopmental disorders such as ADHD and autism spectrum disorder (ASD).[47,110]

1.5.1 Early intervention in neurodevelopmental disorders

Changes in the development or dynamics of the dopaminergic system at any point in life can be an underlying cause of neurodevelopmental disorders.[111] One example is ADHD, where some of the underlying mechanisms are altered dopamine receptor and transporter availability in regions important for attention and impulse control, such as the prefrontal cortex.[112] A PET study showed that receptor density and transporter availability were significantly reduced in patients with ADHD.[113] This decreased density was noticeable in the striatum and prefrontal cortex, areas that are essential for regulating attention and executive functions.[113,114]

One meta-analysis done summarized findings from brain structure and function studies conducted using MRI to test the effects of stimulants on the neurobiology of ADHD patients.[115] The regions of interest in the review were the prefrontal cortex and striatum.[115] Collectively, these studies suggested that psychostimulants, such as methylphenidate and amphetamine, tend to restore brain structure and function in these regions, by blocking the action of DAT or reversing it, respectively.[115] Other studies in this meta-analysis found that treating ADHD patients with psychostimulants initiated restoration of cortical thickness and grey matter volume compared to untreated ADHD patients; functional connectivity that was altered in untreated patients, was also restored partially with the use of psychostimulants.[115]

Normalisation of function after the use of psychostimulants further supports the theory that abnormal changes in the dopamine system contribute to the neurobiology of ADHD.[114,115]

Similar to ADHD, dysregulation in dopaminergic pathways has been linked to ASD. It is believed that changes in communication and social behaviours, as well as the increase in repetitive behaviours observed in ASD are influenced by dopaminergic system malfunctions.[116] This was observed in both animal and human studies.[117] Studies in rodent models showed that disruptions in dopamine signaling affecting the nigrostriatal and mesolimbic pathways were strongly correlated with impaired social behaviours and increased repetitive actions.[118] In addition, blocking D2 receptors reduced repetitive behaviours, the same outcome observed when enhancing the activity of D1 receptors.[118] In humans, neuroimaging studies showed that diminished sensitivity to social reward and motivation in ASD groups correlated with reduced dopamine transporter availability in the striatum.[119,120] Neuroinflammation is also believed to be a contributor to ASD symptoms; One group studies the effects of neuroinflammation on the blood-brain barrier, and its potential effects on the development of ASD symptoms, mainly after seizures caused by neuroinflammation.[116,121,122] This potentially points at a path for therapeutic intervention.[122] The dopamine hypothesis of ASD was revisited, and it was suggested that a dysregulated dopaminergic system, whether overactive or underactive, could be a contributor to some of the core ASD symptoms.[116,121] Over the years, these studies have laid out evidence of the importance of dopaminergic pathways and neuroinflammatory processes in ASD pathology and inform future directions of research and potential treatments.[121–123]

In addition, it is also believed that the motor and vocal tics observed in Tourette's syndrome are associated with dysregulation in the dopaminergic system of the nigrostriatal pathway .[124] These findings reinforce the need for early diagnosis with the help of neuroimaging that can pick up dopaminergic dysfunctions early on, thereby leading to early interventions using behavioural and pharmacological interventions tailored to address dysfunctional aspects of the dopamine systems.[26,110,114,122,124]

1.5.2 Addressing age-related cognitive decline

As individuals age, changes in the dopaminergic system are normal, and contribute to cognitive aging.[125] These changes are manifested by reduced dopamine receptor density, dopamine synthesis, and the loss of dopaminergic neurons, one of the most studied aspects of cognitive aging in the SN.[105,126] There is however, some differences in the onset and extent of neuronal loss with age.[126,127] Differentiating between normal and abnormal neuronal loss could be key in detecting onset and progression of neurodegenerative conditions.[125,127,128] A three-dimensional and stereological study of the human SN during aging highlighted that neuron loss does not happen in a homogenous manner across the SN, but rather specific subregions are more prone to this loss. Specifically, the ventrolateral region showed more pronounced loss than others, potentially explaining the decreased motor performance in older adults.[129] It was also found that dopaminergic neuronal loss could reach up to 50% in the SN by the time individuals are in their eighth decade of life.[129]

Identifying these changes in the dopaminergic system is important both for efforts to develop strategies to mitigate age-related cognitive decline, and for future interpretation of NM imaging as a biomarker for susceptibility of the onset of neurodegenerative disorders or indicator of a healthy aging trajectory.

1.5.3 Previous and current methods for measuring dopamine

Over the past century, neuroscientists have sought to measure dopamine levels in the brain, to gain insights into critical functions of the dopaminergic system and its role in different psychiatric and neurodegenerative conditions.[130–134] Since the discovery of dopamine, different methods have been tested to measure its levels in the brain, with some yielding more detailed information at the cost of being more invasive than others.

1.5.3.1 Early methods

High performance liquid chromatography (HPLC), coupled with electrochemical detection, was one of the methods used to measure dopamine.[130] Due to its sensitivity, this technique allowed for the quantification of dopamine metabolites in the cerebrospinal fluid and blood plasma.[130,131] There are two steps involved in HPLC: first, the sample is passed through a solid absorbent-filled column at high pressure, this causes the separation of components based on their migration times. This is followed by quantification using the electrical current favouring dopamine oxidation or reduction.[130] HPLC had major limitations; the sampling process is destructive, therefore repeated measurements from the same sample were impossible, preventing HPLC from being used in longitudinal studies non-invasively.[130,131]

Microdialysis emerged as another method to measure dopamine.[132] This technique employs a semi-permeable probe that is inserted into the brain tissue to collect extracellular fluid.[132,135] The probe is then perfused with a physiological solution and, as it is passing this solution through the probe, neurotransmitters, including dopamine, collected from the extracellular space are also being picked up.[135] In most cases, HPLC is used to quantify dopamine.[132] Although microdialysis offers real-time tracking of dopamine in the brain and is useful when testing the impacts of behavioural or pharmacological manipulations on dopamine levels, the possibility of tissue damage or inflammation remains high.[132,136] In addition, its invasive use makes it unsuitable for humans as it raises ethical questions in addition to the practical problems of how to insert probes into the human brain for research purposes.[132,137]

1.5.3.2 Advancements in imaging techniques

More recently, new imaging techniques have been developed and validated, representing a new era of diagnostic tools, and helping the enhancement of our understanding of the dopaminergic system.[66,133,134] Among these innovative techniques for the assessment of dopamine are PET and SPECT.[66,133,134] These methods employ radiolabelled catecholamine analogues that bind to dopamine

receptors or transporters to image and quantify key components of the dopaminergic system in the living brain.[138]

PET scans have been widely used in dopamine-related research. They involve the injection of a radiolabeled tracer or ligand such as fluorodopa (^{18}F-DOPA) and [^{11}C]-raclopride, that bind to dopamine receptors or are taken up by dopaminergic neurons.[139,140] When the isotope decays, it emits positrons and high speeds, and these interact with surrounding electrons, creating gamma rays that are eventually detected by the PET scanner.[141] The final images produced by PET show the distribution and concentration of dopamine receptors and transporters in the brain.[141] PET imaging has restructured our understanding of the dopaminergic system in health and disease. It helped shed light in the pathophysiology of several neurodegenerative and psychiatric diseases such as PD and schizophrenia.[142] PET can be used as a measure of dopamine function in addition to its ability to measure receptor and transporter availability.[143,144] For example, dopamine release capacity can be assessed using a [^{11}C]-raclopride scan before and after an amphetamine challenge.[144] A recent PET study investigated the relationship between dopamine synthesis, D2/D3 receptor binding, and dopamine release.[144] The findings of this study showed that there is a strong correlation between dopamine synthesis capacity and D2/3 receptor binding, but did not show any connection with dopamine release.[144] This suggests that dopamine release operates independently from dopamine synthesis and receptor binding, further demonstrating that the dopamine system is more complex than others.[144] A similar approach using ^{18}F-DOPA PET allowed researchers to measure dopamine synthesis capacity.[145] PET techniques were key in showing that decrease dopamine synthesis is observed in PD, and receptor binding is affected in schizophrenia, both underlying conditions causing clinical symptoms and disease progression.[65,146]

SPECT is very similar in principle to PET but uses a different set of radiolabeled ligands, such as [^{123}I]-FP-CIT (DaTSCAN), a dopamine transporter ligand.[147] SPECT photons are emitted directly by the tracer and captured by the SPECT camera to form images.[148] SPECT tends to have a somewhat lower

spatial resolution than PET but is more widely available and less expensive, making it a valuable clinical and research tool.[148]

Both PET and SPECT have numerous limitations, despite their groundbreaking contributions in our understanding of the dopaminergic system.[142,149] Radioactive tracers pose risks of exposure, especially with repeated scans, such as longitudinal studies.[150] In addition, PET involves other invasive procedures like arterial blood collections and some pharmacological challenges.[141] Their use is restricted for research in vulnerable populations such as children or adolescents.[142] In addition, compared to magnetic resonance imaging (MRI), PET and SPECT both have lower spatial resolution, which can cause some challenges when studying smaller brain structures.[151]

Another non-invasive imaging tool that has been used to image dopaminergic activity is functional MRI (fMRI).[152] fMRI can detect changes in blood oxygen related to neural activity, allowing scientists to study activity of brain structures in circuits relevant to the dopamine system.[151,153] This would ideally show up during tasks that involve the processing of rewards, such as the monetary incentive delay task.[154] However, the assumption that fMRI (e.g. in the striatum) reflects dopaminergic activity within the structure has been challenged by some studies.[151] Several groups have demonstrated that fMRI signal correlates to dopamine release in the striatum measured using PET, while others argue that fMRI is a less direct method in measuring dopamine dynamics, demonstrating less specificity than the one seen in PET and SPECT.[151,155]

These limitations have led to the development of new imaging techniques designed to measure dopamine more accurately while being non-invasive. One of the most promising advancements in this regard is NM-MRI.

1.5.4 Neuromelanin-sensitive MRI

1.5.4.1 Neuromelanin synthesis and functions

Neuromelanin (NM) is a byproduct of catecholamines metabolism such as dopamine and norepinephrine.[143,156] It is a dark, insoluble pigment primarily localized in dopaminergic SN neurons and noradrenergic locus coeruleus (LC) neurons, the principal nucleus of the norepinephrine system.[108,157] NM synthesis involves the oxidation of dopamine in the cytosol, followed by the polymerization of dopamine quinones with NM intermediates.[4,3,158] Quinones are highly reactive and can form toxic species.[158,159] However, after further reactions, including interaction and polymerization with proteins and lipids from other organelles, the formation of NM is complete.[157,158] This complex polymer contains various components, including melanin, protein, lipids, and metal ions (Figure 5).[158] NM synthesis occurs over an extended period, leading to the gradual accumulation of NM within neurons.[157,158]

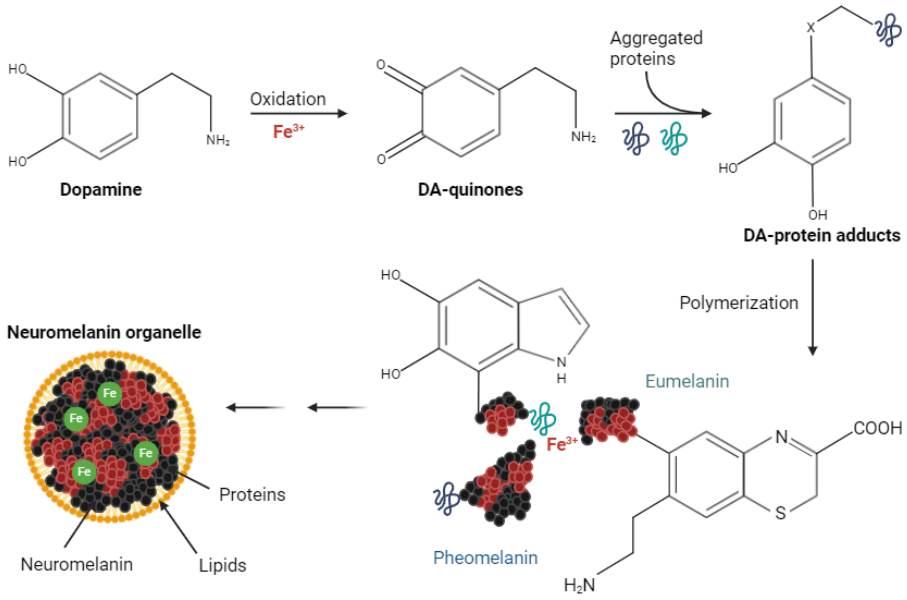

Figure 5. Schematic representation of NM synthesis. *NM is produced through the oxidation of dopamine and its subsequent polymerization.*[158] Created with BioRender.com

NM is known to have a protective role within neurons by binding and sequestering potentially toxic compounds, such as iron, copper, and other heavy metals. [160,158,161] This interaction prevents these

metals from catalyzing the formation of reactive oxygen species (ROS) through Fenton reactions.[162] Consequently, oxidative stress is reduced, and cellular damage leading to neurodegenerative processes is prevented.[161] In addition, some studies highlight the ability of NM to bind to other toxic substances, including pesticides and neurotoxins, protecting neurons from damage.[158,161]

NM is a marker of neuronal metabolic activity and functional integrity.[157] High NM levels in the neurons, which accumulate when the neuron is actively synthesizing and metabolising dopamine over a prolonged period, are an indicator of overall neuronal health.[108,159,160] In a normal, healthy brain, NM accumulation reflects normal neuronal function and longevity.[161] However, changes in NM levels can be associated with various pathological conditions.[158,163] For example, a marked reduction of intraneuronal NM in the SN is well-established in PD patients, indicating a potential neuronal loss in this brain region.[159] In addition to its various roles, NM has been associated with neuroinflammation.[164] Indeed, under pathological conditions associated with neurodegeneration, NM is released from neurons following their death and can interact with the brain's immune cells, the microglia.[164] These can release pro-inflammatory cytokines and other factors that can damage neurons and further worsen neurodegenerative processes.[164] The dual role of NM as a trigger for neuroinflammation and a protective agent portrays NM's complex involvement in the brain.[160]

1.5.4.2 Measuring NM signal using MRI

In recent years, NM has become a suitable visualization and quantification target for advanced imaging methods.[143,156] NM's characteristics and roles make it seem like an advantageous biomarker for researchers and clinicians to assess the integrity and function of the dopaminergic and noradrenergic systems.[143,163] This is useful to study the onset and progression of some neurodegenerative diseases and monitor therapeutic responses non-invasively.[143,163] NM-MRI offers several advantages over traditional imaging methods.[158] These include its use in longitudinal studies since no radioactive tracer is needed,

making this method ideal for studying the progression of some neurodegenerative diseases over long periods of time.[143,163] It also allows monitoring the effects of therapeutic or behavioural interventions over time, even in vulnerable populations like children and adolescents.[158] Moreover, NM-MRI presents a higher spatial resolution than PET and SPECT, making it easier to study dopamine in smaller brain areas, eventually offering a promise to better understand the function and dynamics of the dopaminergic system in the human brain.[156,158,163]

NM-MRI relies on the paramagnetic properties of iron-bound NM to create high-resolution images of NM-containing regions in the brain (Figure 6).[143,158] The NM-MRI sequence depends on a strong magnetic field in combination with radiofrequency pulses.[158] These excite hydrogen nuclei found in water molecules.[165] The relaxation properties of these nuclei differ in NM-rich areas due to the paramagnetic effects of NM, leading to shortening of T1 relaxation.[165] A significant portion of the NM signal is due to magnetization transfer, an effect where the magnetization from one pulse differentially influences the response to a subsequent pulse depending on the ratio of bound to free protons, thereby increasing the contrast in NM-rich areas.[143,156,158,163] This results in distinct signal intensities producing high-resolution images. The contrast shown by NM-MRI highlights regions like the SN and LC where NM is abundant.[143,156,163]

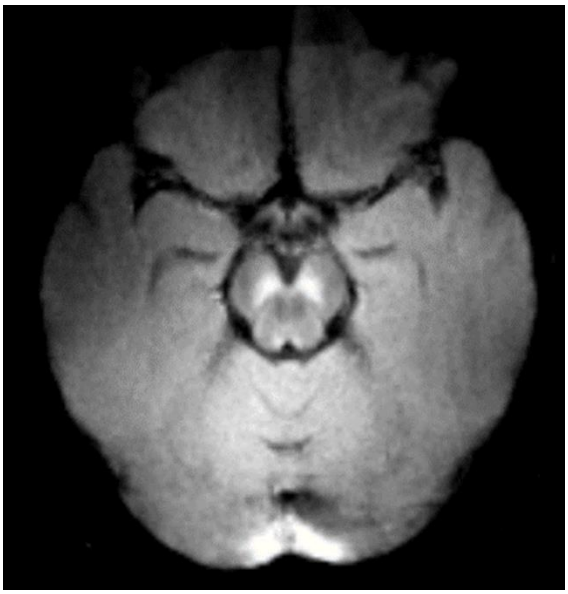

Figure 6. NM-MRI uses NM's paramagnetic properties to create high-contrast images of NM-rich brain regions*. The bright area in the midbrain represents the NM-rich SN (Representative participant scan mage captured using MRICron at the Royal Ottawa Mental Health Centre).*

NM-MRI has transformed the field of neuroimaging of the dopaminergic system. Some studies showed that dopaminergic neuron loss can be detected during early stages of PD, even before the onset of the motor symptoms that are characteristic of this disorder.[163,166] This capability could help in applying therapeutic interventions that can potentially slow the disease progression. Beyond PD, abnormalities in NM levels, even in the absence of degeneration of dopaminergic neurons, have been linked to conditions such as substance use, depression, and schizophrenia.[151,163] Following validation of the use of the method as a measure of dopamine system function, not only degeneration.[143]

1.5.4.3 NM-MRI sequences

This sub-chapter explains the basics behind the two NM-MRI sequences that will be used in this thesis: gradient-recalled echo with Magnetization Transfer (MT, applied in Aims 2, 3, and 4) and Turbo Spin Echo (TSE, applied in Aims 1 and 2). Details of image acquisition, in addition to differences between the two sequences and some of their underlying physics will be elaborated.

Fundamentals of MRI

MRI is known to be a non-invasive imaging technique that uses the magnetic properties of atomic nuclei.[165] The human body is predominantly composed of water, and most MRI implementations target the hydrogen nuclei (protons) found in water molecules.[165,167] Upon the application of a strong magnetic field, the protons align with that field, and when an external radiofrequency (RF) pulse is applied, the alignment of these protons is disrupted.[165] When they return to their equilibrium state, they emit RF signals which are detected by the MRI scanner.[165,168] The main component that constitutes the difference in contrast between different tissues are the relaxation times (T1 and T2) of these protons.[165,169] The MRI scanner processes these signals, creating detailed images of different tissues in the body.[169]

Magnetization Transfer (MT) sequence

The MT sequence uses the interactions between macromolecule-bound protons and free water protons to enhance MRI contrast in different tissues.[170] First, an off resonance RF is applied, saturating the macromolecular-bound protons.[171] Then, a standard RF pulse excites the free water protons through chemical exchange and dipolar coupling, leading to a signal reduction of the free water signal.[168,172] There are two scans involved in forming the MT contrast; one scan with an MT pulse, known as MTon, and another scan without an MT pulse, known as MToff.[168,172,173] The signal from these two scans is subtracted to increase the contrast in areas where free water is dark.[168,172,173] In NM-MRI, water-rich areas appear bright because only the MTon scan is used, which could be part of the reason why some confusion exists regarding the MT effect origin in NM-MRI, considering the fact that the SN is known to have high free water content.[172] This could be due to the known large cell bodies of dopaminergic neurons in this brain region.[172,173] The T1 shortening impact of NM is likely to contribute to the contrast seen in these images, in addition to the MT effect.[172] Paramagnetic substances like NM can influence the relaxation time of the bound pool, further complicating interpretations (Figure 7).[174]

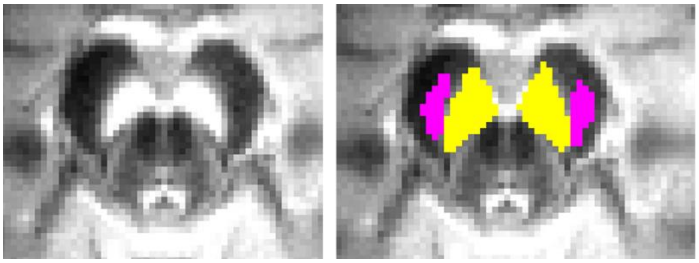

Figure 7. NM-MRI MT scan in standardized space displaying the SN. *The left image shows the SN, while the right image overlays a mask (yellow, 1948 voxels) on the SN to measure CNR, with the pink mask highlighting the Crus Cerebri.*

One of the many aspects that make the MT method advantageous in addition to its short acquisition time, is its high sensitivity to macromolecular content.[169,171]

Turbo Spin Echo (TSE) sequence

Through the repeated application of 180° refocusing pulses following an initial 90° excitation pulse, the TSE sequence, also known as Fast Spin Echo (FSE) sequence, improve MRI images by reducing the effects of magnetic field inhomogeneities and increasing the contrast-to-noise ratio (CNR).[175,176] Several critical steps are followed to acquire the TSE sequence. First, a 90° RF pulse tilts the magnetization into the transverse plane.[175,176] This is followed by a series of 180° refocusing pulses, which generate multiple echo signals.[175,176] Each of these generated echo signals contributes to building a different part of the image in k-space, increasing CNR and image resolution.[177] A major function of the 180° refocusing pulses is correcting for dephasing caused by inhomogeneities in the magnetic field.[152,177,178] The TSE method offers several advantages, including high CNR due to the multiple refocusing pulses, reduced artifacts from magnetic field inhomogeneities, and showing greater anatomical detail (Figure 8).[156,177]

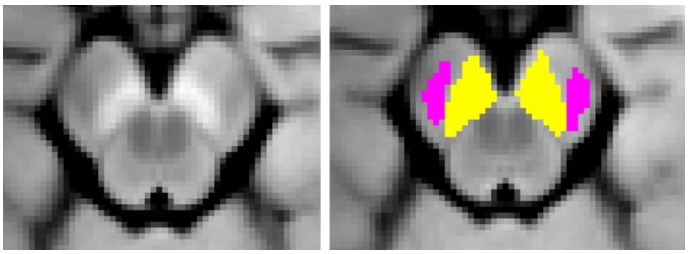

Figure 8. NM-MRI TSE scan in standardized space displaying the SN. *The left image shows the SN, while the right image overlays a mask (yellow, 1948 voxels) on the SN to measure CNR, with the pink mask highlighting the Crus Cerebri.*

1.6 Dopamine research advancement with NM-MRI

1.6.1 Understanding dopamine dynamics

The understanding we have about the development of the dopamine system and its functional dynamics primarily arises from rodent studies.[179] These studies, although very beneficial, do not fully elucidate the dopaminergic system's characteristics in humans, mainly in younger populations.[1,128,180] One step towards a clearer and more comprehensive understanding of the dopaminergic system in humans is exploiting the non-invasiveness and high resolution of NM-MRI to establish the normative ranges of NM-MRI signal throughout the lifespan. Although several PET radiopharmaceuticals have proven their usefulness and accuracy in measuring the dopamine system dynamics, PET's application, especially in vulnerable populations involving children, is limited by the risks associated with repeated pharmaceutical injections.[181,182] This is in addition the cyclotron's high operating cost, and the logistical challenges with short half-life tracers.[181,182]

As previously mentioned, NM accumulates progressively in the SN across the lifespan, reflecting dynamic dopaminergic activity.[128,143,157,183] As it accumulates, NM's slowly changing concentration can be seen as a trait-like measure of cumulative dopamine function throughout life.[143] This was shown in a postmortem study by Zecca et al in 2002, potentially the first study of the absolute NM content in the SN of healthy subjects, plus PD patients.[183] This study reported the concentration of NM in μg/mg SN tissue vs age.[183] It showed a constant increase in NM content in the SN in healthy individuals from 1 to 97 years old.[183] However, this was not the case in PD patients, who exhibited lower NM content in comparison to their age and sex matched healthy peers.[183] This study not only showed that NM is a good marker of SN damage in PD but also establishes a trend of NM accumulation in healthy individuals across the lifespan.

A recent cross-sectional study by Xing et al investigated NM patterns using NM-MRI across a large age range: 5-83 years old.[128] The main finding of this study was that the CNR of the NM signal in SN, both in anterior and posterior parts, increased almost linearly during the first two decades of life.[128] This was followed by a plateau before the signal started decreasing at around 50 years old.[128] Once the normative patterns of NM signal are established, differentiation between normal change in signal due to aging and change underlying pathological conditions becomes possible.[128,156] It is also crucial to understand how other factors such as age, sex and race influence the signal, improving our understanding the pathology of the dopamine system in psychiatric or neurodegenerative populations.

As a relatively newly validated technique to measure NM-MRI signal, it did not yet fully elucidate the demographic factors that might affect the signal; and its high-resolution capability hasn't been fully explored yet. What is currently known, from imaging and post-mortem studies, is that age plays an important role in the NM-MRI signal in the SN.[157,158] The main aim of this project is to refine the methodologies for looking at age effects within the SN, testing if cognitive factors linked to the dopaminergic system affect the signal, and demonstrate that NM-MRI can be used to examine this signal in a clinical group.[158]

Many factors point to the SN as being the main region of interest while looking at the NM-MRI signal to study dopamine dynamics.[156,163] The SN houses the largest part of dopamine neurons present in the brain.[128,129] Significant cognitive impairments were caused by neuronal degeneration in this region, as seen in PD.[161,166,184] These results were shown in both non-human primate models and human data, where dopaminergic neuron loss in the SN was correlated to cognitive dysfunctions.[38,185] PET imaging studies have been essential in establishing the relationship between cognitive performance and dopamine synthesis capacity in healthy individuals.[144,186] An example is a recent study, where direct link between

dopamine levels and cognitive function was found by showing that individual differences in dopamine synthesis capacity were correlated with cognitive performance.[30]

1.6.2 Dopamine and attention deficit hyperactivity disorder

1.6.2.1 Dopamine changes in ADHD

Adolescence is a critical period where psychiatric disorders can develop.[50] This is mainly due to the critical nature and extend of brain development during this period, mainly in areas rich in dopaminergic neurons such as the basal ganglia, which are involved in motor control and reward processing.[81,187] During this maturation phase, attention, behaviour, and executive functions are regulated by dopamine, all of which considered as points of difficulty for ADHD patients.[112] In addition, to the basal ganglia, the prefrontal cortex is affected; this region is essential for executive function such as decision making and impulse control.[187]

In ADHD, dopamine transporter density and receptor availability are altered.[188] The dopamine transporter, responsible for the reuptake of dopamine from the synaptic cleft back to the presynaptic neuron, usually increases in density in ADHD, causing faster clearance of dopamine from the synapse, decreasing dopamine signaling.[188,189] In addition, abnormal changes in the densities of the D2 and D3 receptor subtypes, could potentially disrupt the balance between excitation and inhibition in neural circuits.[190] Studies have shown that reduced D3 receptor availability in the prefrontal cortex is associated with executive function deficits, contributing to the symptoms of ADHD.[92]

These abnormalities affecting the dopaminergic system can be the root cause of the characteristic ADHD symptoms: attention deficit, manifesting in frequent distractibility and difficulty maintaining focus on tasks, and hyperactivity, often presented as inability to sit still and a general sense of restlessness.[50]

1.6.2.2 Pharmaceutical interventions in ADHD

Several strategies have been implemented in the treatment of ADHD.[50,190,191] Pharmacological treatments like stimulant medications (e.g., methylphenidate and amphetamines) and non-stimulant medications (e.g., atomoxetine) work by increasing dopaminergic signalling.[190–192] These strategies have proven effective in reducing hyperactivity, controlling impulsive behaviours, and improving attention in ADHD patients.[190–192] Clinical interventions in ADHD are not only limited to pharmaceutical agents, but also involved behavioural interventions.[193] This includes behavioural parent training, and cognitive-behavioural therapy (CBT), both of which contributing to improved cognitive functions and increasing the ability to develop coping strategies.[194] Other interventions, especially during adolescence, that have shown to be helpful are physical exercise, adequate sleep, and a balanced diet supporting the maturation of dopaminergic pathways.[195,196,197]

1.6.2.3 Using NM-MRI as a tool to better understand dopamine signal in ADHD

Understanding the connection between ADHD and the dopaminergic system highlights the importance of exploiting imaging techniques like NM-MRI to provide information that could lead to better diagnosis and treatment development strategies for ADHD.

NM-MRI yields high-resolution images of the SN, helping to detect functional abnormalities that contribute to the disorder. Since NM-MRI can be used repeatedly, without the risk of being invasive, it could be used to monitor developmental change of the dopaminergic system within an individual, or even perhaps to monitor treatment response, thereby leading to optimization of pharmacological and behavioural interventions strategies to improve outcomes for individuals with ADHD.[143]

The use of NM-MRI in psychiatric and neurodegenerative research in general is still in its early stages, but this technique offers a significant promise.[143] Based on the existing evidence that ADHD is linked to the dopaminergic system, and the ability of NM-MRI to be used to monitor dopamine dynamics,

this advanced imaging technique is essential to exploit.[187,194] NM-MRI's ability to visualize NM in dopaminergic neurons offers unique insights into the structural integrity of these pathways, potentially leading to improved diagnosis, monitoring, and treatment of ADHD.

1.6.3 Missing pieces of the puzzle

Despite our understanding of the dopaminergic system and its involvement in numerous neuropsychiatric and neurodegenerative disorders, some substantial gaps remain. Although traditional methods delivered indispensable data, they were flawed with invasiveness, or spatial resolution, affecting their ability to detect subtle changes in dopaminergic activity. The invasive nature of these methods, PET in particular, prevented researchers from gaining deeper understanding of the role of the dopaminergic system in vulnerable populations, such as children and adolescents, where disorders like ADHD are likely to develop. This is where NM-MRI comes into play. This non-invasive imaging technique, allowing the visualization of dopaminergic neurons in the SN and LC, for example, in high clarity and specificity, may be the tool needed to help close this knowledge gap.

Our study not only exploits the advantages offered by NM-MRI but also employs an advanced detailed analysis method enabling us to look at the SN with a level of precision that previous studies came short of. This capability allows us to highlight anatomical regions within the SN that may have been missed using other imaging methods, potentially helping us understand age-related changes in the dopaminergic system. NM-MRI’s proved robustness is underscored by its high test-retest reliability, which has been demonstrated in several studies.[143,198] This study and others showed that the observed NM-MRI signal changes are actually due to biological factors even in the absence of degeneration of dopamine neurons.[143,198] Our study also incorporates cognitive tasks, offering a more comprehensive understanding of the relationship between cognitive abilities and dopaminergic system integrity.

NM-MRI has promising potential in filling these critical gaps, deepening our understanding into how dopamine dysregulation manifests in the brain, particularly in relation to cognitive tasks. This understanding will help lay the cornerstone for the development of more precise and effective therapeutic strategies.

1.7 Rationale, hypothesis and aims

1.7.1 Rationale

Since NM-MRI has shown to be an efficient and non-invasive method to measure dopaminergic system activity in the human brain, it offers a great tool to enrich our understanding of the complexities of the dopaminergic system. To pave the way for future development and discoveries using NM-MRI, it is first essential to establish the normative range of the NM-MRI signal in healthy individuals. This will be of great advantage, not only in growing our understanding of how the dopamine system develops and to map out what is considered 'normal', but to also see how some demographic factors might affect the signal. Examining the subregional anatomy of the SN may be essential to maximize the utility of NM-MRI but this has been a concept that many previous studies have neglected.

Imagine having the ability to anatomically dissect the SN into small regions, just like separating the pieces of a puzzle. This offers a perception into how each piece of the puzzle contributes to the overall result and allows us to identify and map how a missing or damaged piece can affect the entire puzzle. Looking at the SN in this great level of anatomical detail allows us to gain deeper knowledge on how the SN functions and tells us what goes wrong in disorders like PD and ADHD.

Trying to find a link between the NM-MRI signal and cognitive function adds another layer of complexity and fascination at the same time. Here, we are not only referring to what happens in neurological disorders, but also in healthy individuals, and how the NM-MRI signal affects the levels of cognitive abilities in this group. This helps us explore the underpinnings of cognitive strengths and vulnerabilities of the dopaminergic system.

To summarize, the potential that NM-MRI holds as a tool in revolutionizing our understanding of the dopaminergic system is significant. First by establishing the normative NM-MRI signal range

throughout the lifespan, then by linking the signal to cognitive function, and finally testing how the signal changes in populations with neurological and psychiatric disorders, we can uncover unprecedented dimensions of brain health and disease. The research showed in this thesis is not only about filling knowledge gaps but constitutes a step forward in reaching new horizons in neuroscience.

1.7.2 Hypothesis

Studying the accumulation of NM over the lifespan in different subregions of the SN is possible using NM-MRI. While NM-MRI has been applied to study neurodegenerative disorders in recent years, we hypothesize that it can be used as a tool to measure dopaminergic function in non-degenerative conditions as well, and, specifically, to assay behaviorally relevant aspects of dopamine function during human development. Our study spans from basic methodological questions such as describing the normative range of the NM-MRI signal and its trajectory across the lifespan using different variants of the NM MRI sequence, to confirming the behavioral relevance of this measure by examining dopamine-dependent aspects of cognition, and finally to demonstrating its relevance to dopamine-dependent psychopathology in the case of youth with ADHD. This series of experiments begins to sketch a path towards the use of this neuroimaging technology as a clinical biomarker, and indeed this work was supported in part by an internship with an industry partner, Terran Biosciences, and directly supported the recent clearance of NM-101 software for clinical use by the FDA.

Overall hypotheses:

1. The NM-MRI signal in the SN increases early in life
2. The rate of increase become slower as age progresses
3. Greater NM signal is positively associated with better cognitive performance on dopamine-related tasks such as working memory
4. Youth with ADHD will show deficits in NM signal compared to neurotypical youth

1.7.3 Specific Aims and Hypothesis

1.7.3.1 NM-MRI signal in older adults and method development: First aim

My first aim is to conduct a detailed characterization of the normative range of SN NM-MRI signal and how this signal changes over time in healthy older adults. This aim is crucial because establishing a baseline of what is considered cognitively healthy in the aging population will work as a reference point for identifying deviations associated with neuropsychiatric and neurodegenerative disorders to support subsequent biomarker development of NM-MRI technology.

The data obtained from this study is helpful in method development, allowing for the refinement and validation of NM-MRI analysis techniques. Improved NM-MRI methods will increase our ability to detect and monitor changes in the dopaminergic system in older adults with greater accuracy, thereby ultimately facilitating earlier and more precise diagnoses of neurodegenerative conditions such as ADHD and PD by facilitating the separation from normal aging. This aim has also supported the above-mentioned development of commercial software by Terran Biosciences (NM-101), which received FDA clearance in 2023 (https://www.accessdata.fda.gov/cdrh_docs/pdf23/K230187.pdf).

1.7.3.2 NM-MRI signal starting early life through adulthood: Second aim

The second aim of this thesis is to characterize the developmental trajectories of the NM-MRI signal throughout the lifespan, with particular focus on the younger age range. Examining dopaminergic system changes in young ages helps uncover early patterns of NM deposition in the SN, thereby elucidating normal developmental fluctuation in dopamine turnover that could be related to critical periods of change and plasticity in the dopamine system. This is also critical in improving the capabilities of future studies to precisely control for development effects on NM-MRI and thereby more precisely investigate its association to relevant behavioral and psychopathological measures.

Moreover, this aim will also support researchers in the choice of NM-MRI sequences by providing a comparison between two commonly used sequencesm, determining which one is most suitable for this age range. We hypothesize that NM-MRI signal in the SN increases early in life and the rate of increase become slower as age progresses.

1.7.3.3 Dopamine-related cognitive function and NM-MRI in youth: Third aim

Building on the data obtained from establishing the normative range of the NM-MRI signal throughout the lifespan, the third aim of this research is to study the relationship between the NM-MRI signal and dopamine-related cognitive tasks. This aim extends the findings from the previous aim to show that the pains we are taking to measure NM-MRI signal in the prior aims are justified because this measure is indeed meaningful in the context of healthy development. We will confirm that variability in the NM-MRI signal during early life is associated with behaviors relevant to the dopamine system such as working memory. We hypothesize that greater NM signal is positively associated with better working memory performance.

1.7.3.4 Dopamine in ADHD: Fourth aim

Once normative developmental trajectories and associations of cognition with the NM-MRI signal have been established, the fourth aim is to translate this knowledge to confirm that NM-MRI can track behavior, not only in health, but also in the psychiatric conditions. This aim compares the signal in the SN of healthy children and adolescents with ADHD compared to age-matched healthy controls. We hypothesize that ADHD patients will have lower NM-MRI signal compared to neurotypical youth. By focusing on children and adolescents, we can detect abnormal changes potentially early in ADHD onset and pave the way to create better interventions that could be more effective in the early stages of the disorder, for instance by optimizing the dose of psychostimulants based on an individual's NM-MRI signal.

Chapter 2: Materials and methods

2.1 Materials and methods for aim 1

2.1.1 Participants

Imaging and non-imaging data for this aim were collected by our collaborators at the McGill Centre for Studies in Aging, specifically from the Translational Biomarkers in Aging and Dementia (TRIAD) cohort under the direction of Pedro Rosa-Neto. All data collected under the TRIAD cohort is governed by the policies set by the Research Ethics Board Office of McGill University, Montreal, and the Douglas Research Center, Verdun.

Upon receiving Research Ethics Board approval, participants from the community were enrolled in the study. After giving written informed consent, participants underwent a detailed clinical assessment, which included the Clinical Dementia Rating Scale (CDR) and the Mini-Mental State Examination (MMSE), administered at baseline and during follow-up assessments.[156] All study participants were cognitively unimpaired, with no objective cognitive impairment and a CDR score of 0. Exclusion criteria included the presence of inadequately treated conditions, active substance abuse, recent head trauma, major surgery, or MRI safety contraindications. A sample of 152 participants (aged 53–86 years) was enrolled for baseline scanning, and 41 participants returned for their follow-up scan approximately 9–16 months after the initial scan.

2.1.2 MRI acquisition

All neuroimaging data were acquired using a 3 T Prisma-Fit scanner (Siemens, Erlangen, Germany). NM-MRI images were collected using a TSE sequence with the following parameters: repetition time (TR) = 650 msec; echo time (TE) = 10 msec; flip angle = 120°; turbo factor = 4; in-plane resolution = 0.6875 ×

0.6875 mm²; partial brain coverage overlaying the pons and midbrain with a field of view (FoV) = 165 × 220 mm²; number of slices = 20; slice thickness = 1.8 mm; number of averages = 7; acquisition time = 8.45 minutes. The image stack was aligned perpendicular to the axis of the pontine brainstem, ensuring coverage from the posterior recess of the fourth ventricle at the caudal extent to a point slightly above the floor of the third ventricle at the rostral extent.

Whole-brain, T1-weighted MR images (resolution = 1 mm, isotropic) were acquired using an MPRAGE sequence for preprocessing of the NM-MRI. The quality of MRI images was visually inspected for artifacts immediately upon acquisition by experienced MR technologists.

2.1.3 Preprocessing of NM-MRI images

Preprocessing of NM-MRI images was performed using a fully automated, cloud-based software package, NM-101, version 1.0.3 (Terran Biosciences, New York, NY, USA). Initial algorithm steps necessary for processing SN metrics included brain extraction of T1-weighted images, spatial normalization of T1-weighted images into standardized MNI space, rigid coregistration of NM-MRI images to T1-weighted images, and spatial normalization of NM-MRI images into MNI space, resampled at 1 mm isotropic resolution. All steps for calculating SN metrics were fully automated.

To calculate SN metrics from the spatially normalized images, we used an approach adopted by Wengler et al. This approach ensures that the SN mask also includes the dopaminergic VTA, thus the structure assayed here is referred to as the SN. Intensity normalization determined CNR for each subject and voxel as the relative change in NM-MRI signal intensity from a reference region RR of white matter tracts, the crus cerebri, known to have minimal NM content[143]:

$$\mathrm{CNR} = \frac{SN\ signal - RR\ signal}{RR\ signal}$$

Images were then spatially smoothed with a 1-mm full-width-at-half-maximum Gaussian kernel. An overinclusive mask of the SN in MNI space was applied to ensure inclusion of the SN and VTA for all individuals. SN signal was calculated by averaging CNR values for all SN voxels on the left and right sides of this mask. SN volume on the left and right sides was calculated by automated threshold-based segmentation, identifying SN voxels in MNI space above a fixed intensity threshold, and multiplying by the volume of one voxel (1 mm^3). The intensity threshold was equal to two times the standard deviation calculated from all reference region voxels of all subjects after trimming reference region voxels with extreme intensity values.

2.1.4 Statistical analysis

All NM-MRI metrics generated by the NM-101 software were analyzed using MATLAB software. Normality was assessed using the Lilliefors test with an alpha level of 0.05. Linear regression was employed to relate both baseline and change in NM-MRI metrics to age. The NM signal was used as a dependent variable, and age was used as an independent variable. Change metrics for all NM-MRI parameters were calculated by subtracting the baseline values from the follow-up values, obtained 9–16 months later. To determine if these change metrics significantly differed from zero, one-sample t-tests were conducted.

2.2 Materials and methods for aim 2

2.2.1 Participants

Imaging and non-imaging data for this aim were collected at the Royal Ottawa Mental Health Center, with data collection carried out by myself, supported by the Cassidy lab and the Brain Imaging Centre. All data collected under the NM-Life (NMLife) cohort is governed by the policies set by the Research Ethics Board Office of the Royal Ottawa Hospital.

Upon receiving Research Ethics Board approval, participants from the community were enrolled in the study. After giving written informed consent, participants over the age of 17 underwent a structured clinical interview for DSM-5® (Diagnostic and statistical manual of mental disorders). Participants were excluded if they had any current psychiatric disorders or lifetime psychotic disorders. Additional exclusion criteria included the presence of inadequately treated conditions, active substance abuse, recent head trauma, major surgery, or MRI safety contraindications. A sample of 119 participants (aged 6 - 82 years) was enrolled for the study.

2.2.2 MRI acquisition

For this aim, two types of NM-MRI sequences were collected. All neuroimaging data were acquired using a 3T Siemens Biograph MR-PET scanner (Siemens, Erlangen, Germany). NM-MRI images were collected using a 2D gradient-recalled echo sequence with magnetization transfer pulse (2D-GRE with MT) sequence with the following parameters: repetition time = 639 msec; echo time = 3.97 msec; flip angle = 50°; in-plane resolution = 0.639 x 0.639 mm^2; partial brain coverage with FoV = 166 x 224; matrix = 260 x 352; number of slices = 24; slice thickness = 1.5 mm; magnetization transfer frequency offset = 1200 Hz; number of excitations (NEX) = 5, acquisition time = 7 minutes. Whole-brain, T1-weighted MR images (resolution = 1 mm, isotropic) were acquired using an MEMPRAGE sequence. The image stack

was aligned perpendicular to the axis of the pontine brainstem, ensuring coverage from the posterior recess of the fourth ventricle at the caudal extent to a point slightly above the floor of the third ventricle at the rostral extent. A total of 119 participants completed the MT scan.

In addition, more NM-MRI images were collected using a TSE sequence with the following parameters: repetition time (TR) = 650 msec; echo time (TE) = 10 msec; flip angle = 120°; turbo factor = 4; in-plane resolution = 0.6875 × 0.6875 mm^2; partial brain coverage overlaying the pons and midbrain with a field of view (FoV) = 165 × 220 mm^2; number of slices = 20; slice thickness = 1.8 mm; number of averages = 7; acquisition time = 8.45 minutes. The image stack was aligned perpendicular to the axis of the pontine brainstem, ensuring coverage from the posterior recess of the fourth ventricle at the caudal extent to a point slightly above the floor of the third ventricle at the rostral extent. A total of 114 participants completed the TSE scan.

Whole-brain, T1-weighted MR images (resolution = 1 mm, isotropic) were acquired using an MEMPRAGE sequence for preprocessing of the NM-MRI data. The quality of MRI images was visually inspected for artifacts immediately upon acquisition by experienced MR technologists.

2.2.3 Preprocessing of NM-MRI images

NM-MRI scans were preprocessed using SPM12 to allow for voxelwise analyses in standardized MNI space. NM-MRI scans were coregistered to T1-weighted scans and normalized into MNI space following the transforms generated for the T1 images using ANTs software.[199] The resampled voxel size of unsmoothed, normalized NM-MRI scans was 1 mm, isotropic. All images were visually inspected after each preprocessing step. Intensity normalization and spatial smoothing were then performed using custom Matlab scripts. CNR for each subject and voxel *v* was calculated as the relative change in NM-MRI signal intensity I from a reference region RR of white-matter tracts known to have minimal NM content, the crus cerebri,[143] as:

$$\mathrm{CNR}_v = \frac{\mathrm{I_v} - \mathrm{mode}\,(\mathrm{I_{RR}})}{\mathrm{mode}\,(\mathrm{I_{RR}})}$$

A template mask of the reference region in MNI space was adapted from our previous work by manual tracing on a template NM-MRI image created from study participants. We ensured this mask was suitable for both MT and TSE NM-MRI images. The mode I_{RR} was calculated for each participant from kernel-smoothing-function fit of a histogram of all voxels in the mask. We employed the mode rather than mean or median because we found it was more robust to outlier voxels (e.g., due to edge artifacts), alleviating any need for further modification of the reference-region mask. Images were then spatially smoothed with a 1-mm full-width-at-half-maximum Gaussian kernel. Finally, an overinclusive mask of SN voxels was created by manual tracing on the template NM-MRI image. This was also adapted from our prior work to be suitable to this study spanning the lifespan and including both MT and TSE sequences.

2.2.4 Statistical analysis

All analyses were carried out in Matlab (Mathworks)using custom scripts. In general, robust linear regression analyses were performed across subjects for every voxel *v* within the SN mask, as:

$$CNR_v = \beta_0 + \beta_1 \,.\, measure\ of\ interest + \sum_{i=2}^{n} \beta_1 \,.\, nuisance\ covariate + \varepsilon$$

Robust linear regression was used to minimize the need for regression diagnostics in the context of mass-univariate, voxelwise analyses. Voxelwise analyses were carried out within the template SN mask. Hypothesis testing was based on a permutation test in which the measure of interest was randomly shuffled with respect to CNR. This test corrected for multiple comparisons by determining whether an effect's spatial extent was greater than would be expected by chance ($p_{corrected} < 0.05$; 10,000 permutations). On each iteration, the order of the values of a variable of interest was randomly permuted across subjects (and maintained for the analysis of every voxel within the SN mask for a given iteration of

the permutation test, accounting for spatial dependencies). This provided a measure of spatial extent for each of 10,000 permuted datasets, forming a null distribution against which to calculate the probability of observing the spatial extent of the effect in the true data by chance ($p_{corrected}$). Partial correlation coefficients from analyses including mean NM-MRI signal (from the whole SN ROI or from sets of voxels identified via voxelwise analysis) were reported, together with their 95% CIs, calculated using bootstrapping.

For this aim, we also performed quadratic regression to examine non-linear relationships. This allowed us to capture the age at which the NM signal in each voxel reaches its maximum value.

$$CNR_v = \beta_0 + \beta_1 \,.\, measure\ of\ interest + \beta_2 \,.\, (measure\ of\ interest)^2 + \sum_{i=3}^{n} \beta_1 \,.\, nuisance\ covariate + \varepsilon$$

Voxels that fit the linear model were interpreted as peaking either at birth (age 0) or after death, signaling no peak during the lifespan.

2.3 Materials and methods for aim 3

2.3.1 Participants

Similar to aim 2, data collection for this aim also took place at the Royal Ottawa Mental Health Centre. However, participants for this aim were all under 18 years of age. A total of 36 participants completed the cognitive and imaging measures.

2.3.1.1 Cognitive measures

Cognition was assessed using tests selected from the NIH Toolbox cognition battery, administered on a tablet. These tests were chosen due to their strong dependence on the dopamine system.

The NIH Toolbox was used to assess cognitive performance through a List Sorting Working Memory (LSWM) task. During this task, participants are presented with a series of pictures of food and/or animals, accompanied with verbal stimuli (i.e. name of the object they are shown on the iPad). The task is to verbally sort them in a specific order, smallest to largest in this case. As the task progresses, participants may by asked to sort two separate lists simultaneously. The task becomes progressively more difficult as it progresses and when the additional list is added.

Scoring for the LSWM task is based on the number of correct trials, where participants correctly recall and sort all items in the list(s). Points are only given when the entire sequence correct, there is no additional time for quicker responses, and no partial points are awarded for incomplete or partially incorrect responses. The final score is the sum of correct responses across all sequences, and both lists if applicable, yielding a measure of the participant's working memory performance. Raw scores can be converted to standardized scores using normative data, enabling comparisons across different age groups and populations.

Previous studies have demonstrated the reliability of these tasks. One study with 89 participants (aged 20-85) showed an Intraclass Correlation Coefficient (ICC) of 0.77 for age corrected LSWM scores over two sessions separated by 7-21 days.[200] Another study with 66 younger participants (aged 3-18) showed ICC values close to 0.86.[201] These findings confirm that the NIH Toolbox LSWM test is normed and validated for individuals across the lifespan and this test has been used in other large neuroimaging studies of youth such as the Adolescent Brain Cognitive Development study.

Other non-imaging measures were collected for this aim, but for the sake of this PhD project, we are only focusing on the LSWM collected via the NIH toolbox.

2.3.1.2 Psychopathology and substance use measures

To assess dimensional psychopathology and adaptive functioning in children (6-12 years old) and adolescents (13-17 years old), parents were asked to complete the Child Behaviour Checklist (CBCL). Participants over 18 years of age underwent a structured clinical interview for DSM-5® (SCID). If there was a potential concern that a participant might have a mental health condition based on CBCL scores (greater than 75 on any sub-domain), families were offered a list of local mental health/family resources. A trained mental health practitioner (Dr. Philippe Robaey) was available as needed to support and refer these families to these resources. Notably, the recommended threshold scores were raised slightly (by 5 points, from 70 to 75) to minimize excessive concern in cases where a participant might have only mild to moderate symptoms.

2.3.2 Statistical analysis

The image acquisition and processing for this aim was identical to aim 2 since this was the same cohort used for both aims. The NM-MRI signal was correlated with cognitive measures using linear regression to predict baseline signal levels. Working memory scores were used as the dependent variable,

and NM signal was used as an independent variable. Covariates included age and sex. All analyses were conducted for both the whole SN and voxelwise within the SN, using MATLAB for statistical computations.

2.4 Materials and methods for aim 4

2.4.1 Participants

Similar to aims 2 and 3, data collection for this aim was conducted at the Royal Ottawa Mental Health Centre. However, this aim exclusively focused on participants under 18 years old and also included youth diagnosed with ADHD. The ADHD diagnosis was confirmed either through medical reports or referrals from our collaborators in Dr. Philippe Robaey's specialized clinic for ADHD and disruptive behavior at the Children's Hospital of Eastern Ontario (CHEO) research institute.

A total of 53 participants, 15 of them with confirmed ADHD diagnosis, completed the MRI scans and the cognitive task LSWM assessment using the NIH Toolbox iPad application. The imaging measures and non-imaging measures were the same as the ones described in aim 2.

2.4.2 Statistical analysis

All NM-MRI metrics generated by the NM-101 software were analyzed using MATLAB software. Normality was assessed using the Lilliefors test with an alpha level of 0.05. Linear regression was employed to relate baseline NM-MRI metrics to age. The NM signal was used as a dependent variable, and age was used as an independent variable. To determine if these change metrics significantly differed from zero, one-sample t-tests were conducted.

The NM-MRI signal was correlated with cognitive measures using linear regression to predict baseline signal levels. Working memory scores were used as the dependent variable, and NM signal was used as an independent variable. Covariates included age and sex. All analyses were conducted for both the whole SN and voxelwise within the SN, using MATLAB for statistical computations.

Chapter 3: Normative values of NM-MRI signal in older adults using a TSE sequence

This chapter shows the results obtained in the first aim of my thesis and establishes the normative values for NM-MRI metrics in older adults using a TSE sequence. The results serve as a reference for clinical and research applications in aging and neurodegenerative studies. The results of this chapter were crucial for the development of a new commercial software strengthening the accuracy and utility of NM-MRI.

3.1 Normative metrics: baseline

The sample comprised 152 adults aged between 53 and 86 years at baseline, with a mean age of 71.2 ± 5.9 years. The mean years of education was 15.3 ± 3.5, and the mean score on the MMSE was 29.2 ± 1.4. Fifty participants were male (32.9%), and 110 participants were Caucasian (86.6%). Baseline SN signal had CNR values of 10.02% (left SN) and 10.28% (right SN), (see Table 1 for all signal and volume measures).

All signal measures were normally distributed at baseline (Lilliefors test, alpha > 0.05). However, not all volume measures were normally distributed, consistent with our decision to set volume thresholds where many healthy individuals would be at or near the ceiling. Figure 9 shows an SN map illustrating voxelwise values for baseline SN signal.

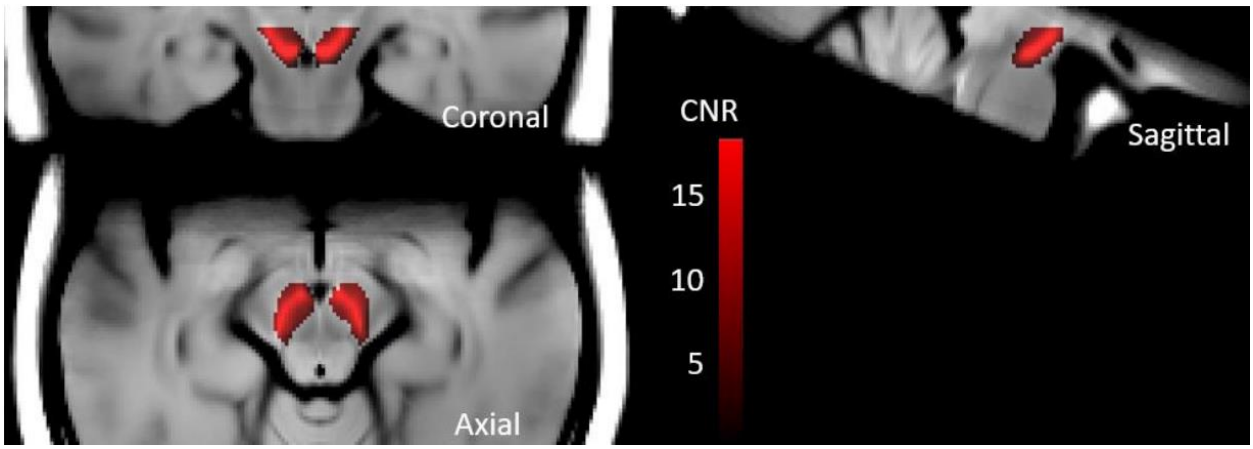

Figure 9. Mean NM-MRI signal from SN voxels at baseline in older adults. *The figure illustrates the mean NM-MRI signal from SN voxels at baseline in older adults, highlighting that the signal is highest in the central SN.*

To determine normative NM-MRI metrics from a relatively broad age range, we examined whether there was meaningful variation in these metrics over this range. Our analysis confirmed no significant relationship between NM-MRI signal or volume in the SN and age (p-values ranged from 0.14 to 0.99, linear regression analysis). This supports the acceptability of the broad age range and is consistent with evidence that age-related changes in NM-MRI metrics plateau in later life.

3.2 Normative metrics: annual change

Follow-up scans were available for 41 participants. The follow-up intervals varied between 9 and 16 months. The mean change in NM-MRI metrics over the year showed a general decrease for SN metrics (Table 1). Just like the observations seen at baseline, annual changes in signal metrics were normally distributed, while changes in volume measures were not. Only the left SN volume showed a significant annual change across participants (Table 1, 1-sample t-tests).

Table 1. Summary of NM-MRI metrics at baseline and change over 1 year.

		Baseline	*Annual change*	*T stat (annual change)*
Signal (CNR)	Left	10.02±1.48	-0.39±1.32	-1.89
	Right	10.28±1.51	-0.30±1.18	-1.61
Volume (mm^3)	Left	576.4±83.0	-30.44±75.9	-2.57*
	Right	540±74.9	-17.21±64.2	-1.72

*p=0.014

We also investigated whether age significantly affected the annual change metrics and found that it did not (p-values ranged from 0.16 to 0.96, linear regression analysis). This suggests that, similar to baseline metrics, combining older adults across this wide age range is acceptable when considering annual change metrics.

Chapter 4: Investigating the NM signal across the lifespan with a focus on young age groups

This chapter shows the results generated for my second aim and explores the variations in NM signal across the lifespan, with a particular focus on the younger population. Detailed anatomical analysis of the SN using voxelwise analysis reveals the developmental patterns of NM signal changes throughout life. This chapter also provides a comparison of two NM-MRI sequences, MT and TSE.

4.1 Age effects, lifespan, MT version

The study cohort consisted of 119 participants ranging in age from 6 to 82 years old each screened to ensure they had no current psychiatric disorders or a history of lifetime psychotic disorders, providing a broad spectrum of developmental and aging stages to analyze. Participants data can be found in Table 2. Age was not different across sexes ($t = -1.11$, $p = 0.27$).

Table 2. Demographic information for participants who completed the MT NM-MRI scan.

MT scan	
Participants	n = 119
Age range	6 - 82 years old
Mean age	33.94±20.36
Males	48.74%
Females	51.26%

4.1.1 Whole SN NM signal analysis

Initial linear regression analysis aimed to correlate the average NM-MRI signal of the whole SN with age, while controlling for sex. The results indicated that there was no significant correlation between age and the NM signal when considering the SN as a whole ($t_{116} = -1.22$, $p = 0.23$). This suggests that, when

viewed as a single entity and using an MT sequence for NM-MRI, the SN does not exhibit a uniform pattern of NM signal change with age (Figure 10). This supports the need to look at subregions of the SN to find age-dependent effects when looking across the lifespan with an MT sequence.

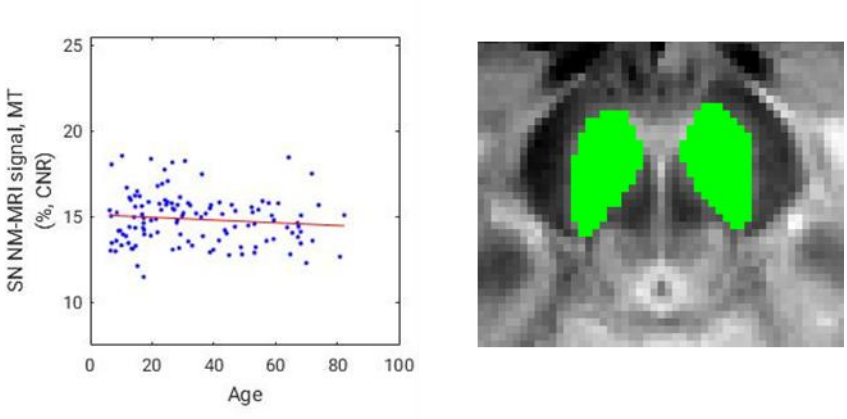

Figure 10. NM-MRI signal of the whole SN, MT version. *No significant correlation between age and SN signal while controlling for sex. The scatter plot shows the relationship between age and NM-MRI signal (CNR) in the SN. The image on the right shows an axial view of the brain with the SN highlighted in green. The highlighted areas indicate where the NM signal was measured.*

4.1.2 Voxelwise analysis of age-related changes

4.1.2.1 Exploration of linear relationships

To achieve a more detailed understanding, a voxelwise analysis was conducted. The voxelwise analysis revealed significant clusters of voxels where NM signal either increased or decreased with age.

Specifically, a cluster comprising 385 out of 1948 voxels exhibited a significant increase in NM signal with age (at a height threshold of $p = 0.05$, cluster-size $p_{corrected} = 0.0110$). This cluster represents regions within the SN where NM accumulation becomes more pronounced as individuals age (Figure 11).

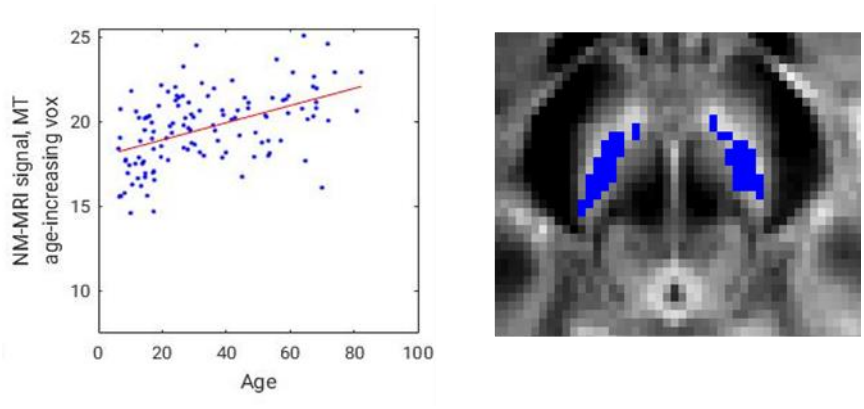

Figure 11. NM-MRI signal of age-increasing voxels (MT version). *385 out of 1948 voxels showed significant increase in signal with age. The image on the right shows an axial view of the brain with the age-increasing voxels highlighted in blue.*

On the other hand, a separate cluster of 556 out of 1948 voxels showed a significant decrease in NM signal with age (at a height threshold of p = 0.05, cluster-size $p_{corrected}$ = 0.0014). This decrease may indicate regions within the SN that undergo a reduction in NM content, potentially due to age-related degeneration of dopaminergic neurons or (Figure 12).

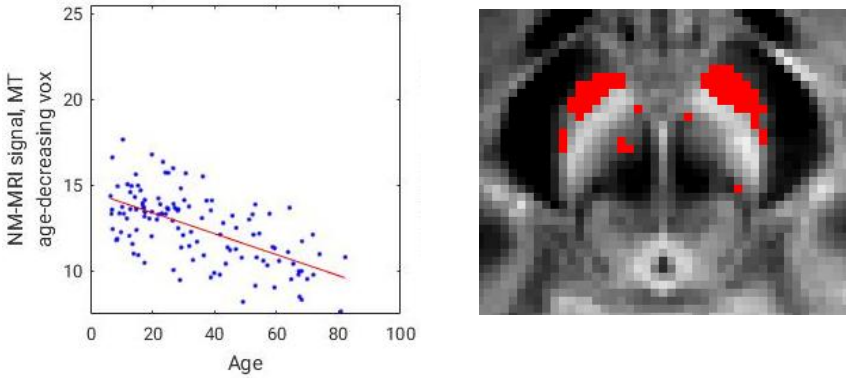

Figure 12. NM-MRI signal of age-decreasing voxels (MT version). *556 out of 1948 voxels showed significant decrease in signal with age. The image on the right shows an axial view of the brain with the age-increasing voxels highlighted in red.*

4.1.2.2 Exploration of Non-linear relationships

In addition to examining linear relationships, we explored the possibility of a quadratic (inverted U-shaped) relationship between age and NM signal within the SN.[128]

This hypothesis was tested using a quadratic term for age in the linear regression model, with a linear age term and sex also included in the model. The analysis of the whole SN did not provide significant evidence for an inverted U-shaped relationship (t_{115} = -1.08, p = 0.28).

However, voxelwise analysis identified a cluster of 304 out of 1948 voxels where a negative quadratic fit for age was significant (at a height threshold of p = 0.05, cluster-size $p_{corrected}$ = 0.035). These results suggest that in specific subregions of the SN, the NM signal increases to a peak around age 40 before declining (Figure 13).

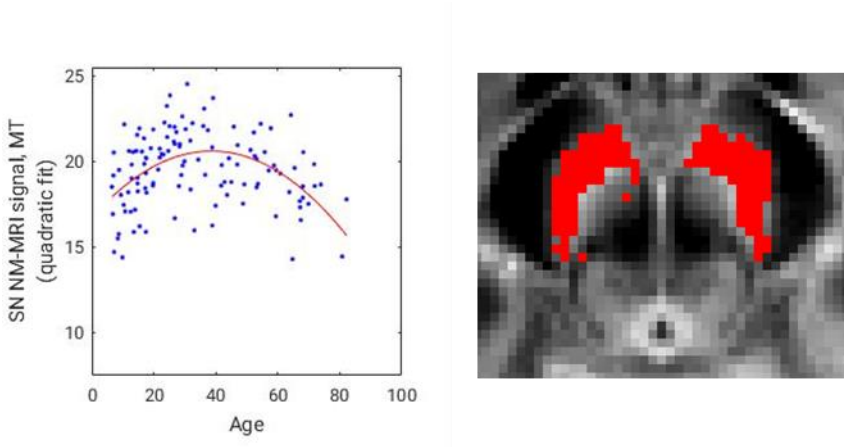

Figure 13. NM-MRI signal of voxels showing an inverted U-relationship with age (MT version). *304 out of 1948 voxels showed significant quadratic fit. The image on the right shows an axial view of the brain with these voxels highlighted in red.*

4.2 Age effects, lifespan, TSE version

The study cohort consisted of 114 participants aged 6 to 82 years, each screened to ensure they had no current psychiatric disorders or a history of lifetime psychotic disorders. Participants data can be found in Table 3. This wide age range provided a comprehensive spectrum of developmental and aging stages for analysis, allowing for a thorough examination of NM signal variations across the lifespan.

Table 3. Demographic information for participants who completed the TSE NM-MRI scan.

TSE scan	
Participants	n = 114
Age range	6 - 82 years old
Males	49.12%
Females	50.88%

4.2.1 Whole SN NM signal analysis

Initial linear regression analysis, controlling for sex, revealed a significant correlation between age and the NM-MRI signal in the whole SN ($t_{111} = 5.36$, $p = 5x10^{-7}$) (Figure 14). This finding indicates a robust age-related increase in NM signal when considering the average SN signal as measured using a TSE sequence, consistent with NM accumulation throughout the SN over the full lifespan.

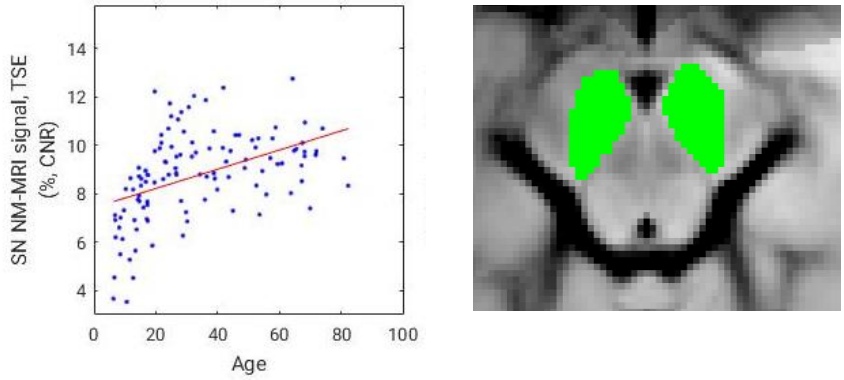

Figure 14. NM-MRI signal of the whole SN, TSE version. *A significant correlation was found between age and SN signal while controlling for sex. The scatter plot shows the relationship between age and NM-MRI signal (CNR) in the SN. The image on the right shows an axial view of the brain with the SN highlighted in green. The highlighted areas indicate where the NM signal was measured.*

4.2.2 Voxelwise analysis of age-related changes

4.2.2.1 Exploration of linear relationships

To gain a more detailed understanding, a voxelwise analysis was conducted (Figure 15). The voxelwise analysis revealed that the majority of SN voxels, specifically 1118 out of 1948, exhibited a significant increase in NM signal with age (at a height threshold of $p = 0.05$, cluster-size $p_{corrected} < 0.0001$).

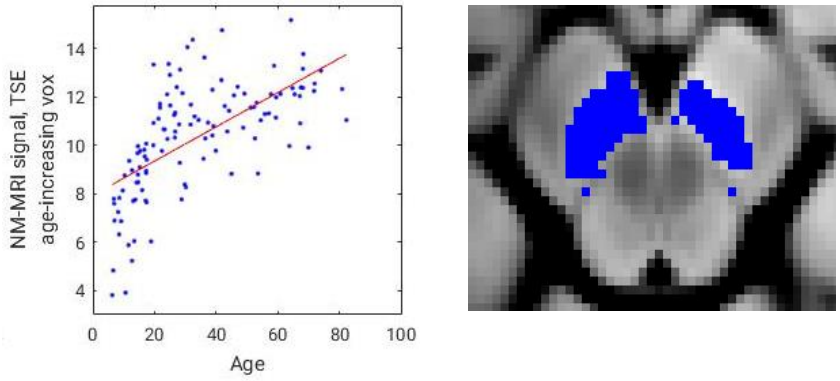

Figure 15. NM-MRI signal of age-increasing voxels (TSE version). *1118 out of 1948 voxels showed significant increase in signal with age. The image on the right shows an axial view of the brain with the age-increasing voxels highlighted in blue.*

However, only a few voxels, 84 out of 1948, showed a significant decrease in NM signal with age (at a height threshold of $p = 0.05$, cluster-size $p_{corrected} = 0.356$). This limited number of decreasing voxels

indicates that reductions in NM content are relatively rare within the SN using a TSE sequence and do not significantly impact the overall age-related trend of increasing NM signal throughout the SN over the entire lifespan (Figure 16).

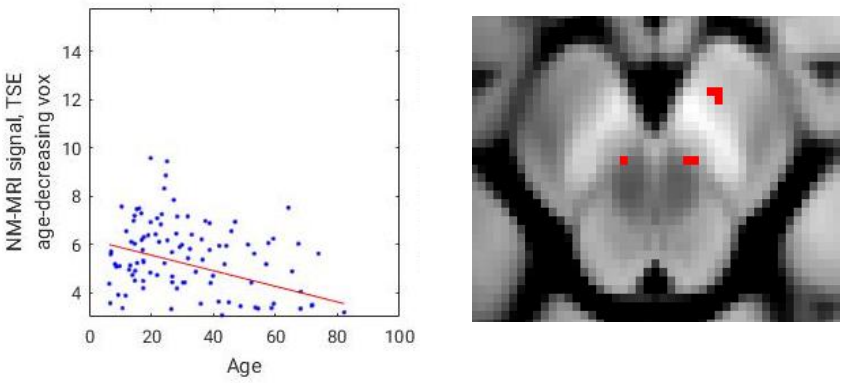

Figure 16. NM-MRI signal of age-decreasing voxels (TSE version). *84 out of 1948 voxels showed decrease in signal with age. The image on the right shows an axial view of the brain with the age-increasing voxels highlighted in red.*

4.2.2.2 Exploration of Non-Linear Relationships

In addition to examining linear relationships, we explored the possibility of a non-linear (inverted U-shaped) relationship between age and NM signal within the SN. This hypothesis was tested using a quadratic term for age in the linear regression model, with a linear age term and sex also included in the model. The analysis showed significant evidence for an inverted U-shaped relationship in the whole SN (t_{110} = -5.44, p =3x10^{-7}). This finding suggests that NM signal increases to a peak at a certain age before declining, indicating complex age-related dynamics in NM accumulation.

Voxelwise analysis supported this non-linear relationship, identifying 1192 out of 1948 voxels where a negative quadratic fit for age was significant (at a height threshold of p = 0.05, cluster-size $p_{corrected}$ = 0.0001) (Figure 17).

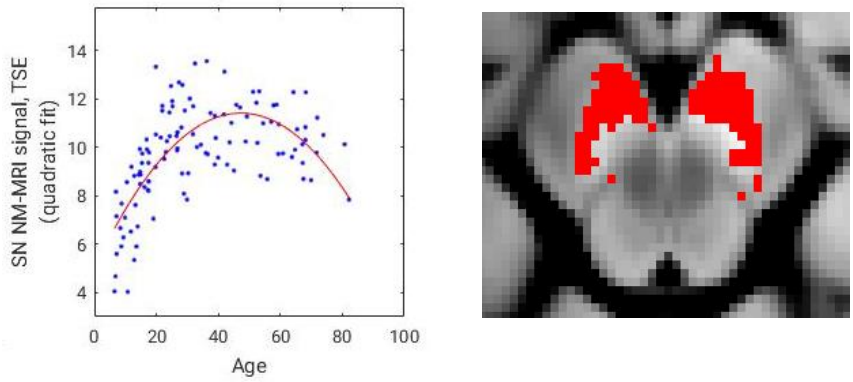

Figure 17. NM-MRI signal of voxels showing an inverted U-relationship with age (TSE version). *1192 out of 1948 voxels showed significant quadratic fit. The image on the right shows an axial view of the brain with these voxels highlighted in red.*

4.3 Age effects, early life, MT version

The study cohort consisted of a subsample of 63 participants under 30 years old. Detailed participant data can be found in Table 5.

Table 4. Demographic information for young participants who completed the MT NM-MRI scan.

MT scan	
Participants	n = 63
Age range	6 - 29 years old
Mean age	12.50±3.63
Males	31.75%
Females	68.25%

Whole SN analysis revealed no significant overall effect of age on NM-MRI signal (t_{60} = 1.49, p = 0.14, linear regression controlling for sex). However, voxelwise analysis identified a significant cluster of 434 out of 1948 voxels, with $p_{corrected}$ = 0.0075, where NM-MRI signal increased by 0.18 CNR units per year. Assuming a linear effect from birth, the signal in this cluster at birth would be approximately 16.9 CNR units (Figure 18). Conversely, a smaller cluster of 28 out of 1948 voxels showed a significant decrease in signal (p = 0.01). There was no significant SN cluster where a sex effect was present (one cluster of 175 out of 1948 voxels showed higher signal in females, one cluster of 101 voxels showed a positive age by sex interaction, all pcorrected>0.05).

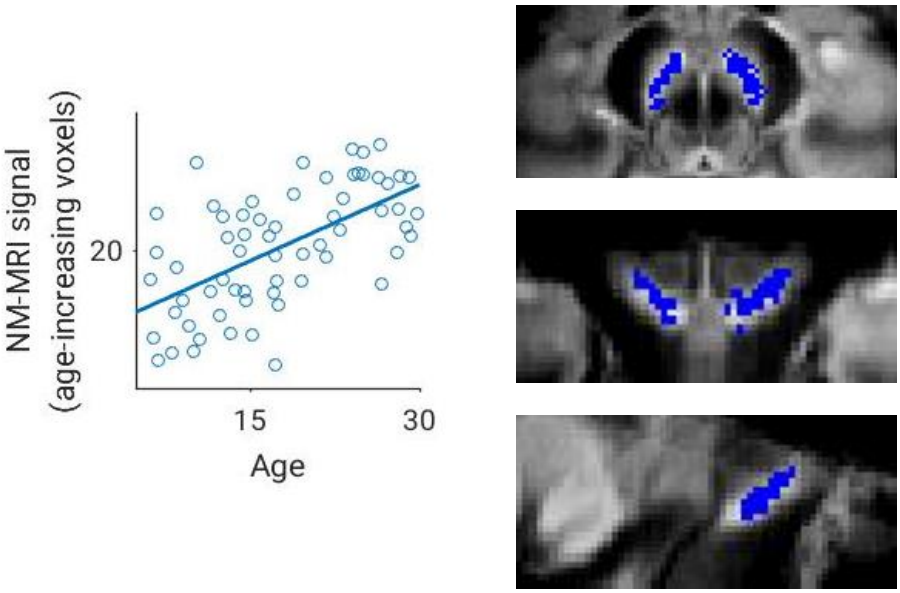

Figure 18. Voxelwise analysis of the NM-MRI signal in early life (MT version). *The left panel shows a scatter plot of NM-MRI signal from age-increasing voxels against age. The right panels display the clusters in the SN (axial, coronal and sagittal views, descending order) where the NM-MRI signal significantly increased with age in younger participants.*

4.4 Age effects, early life, TSE version

The study cohort consisted of 60 participants under 30 years old. Detailed participant data can be found in Table 4.

Table 5. Demographic information for young participants who completed the TSE NM-MRI scan.

TSE scan	
Participants	n = 60
Age range	6 - 29 years old
Mean age	12.58±3.71
Males	31.67%
Females	68.33%

Whole SN analysis revealed a significant overall effect of age on NM-MRI signal (t_{57} = 6.47, p = $2x10^{-8}$, linear regression controlling for sex). Voxelwise analysis identified a significant cluster of 1541 out of 1948 voxels ($p_{corrected}$ = 0.0001) where the NM-MRI signal increased with age across this range. The signal in this cluster increased by 0.18 CNR units per year, and assuming a linear effect from birth, the signal in this cluster at birth would be approximately 5.0 CNR units (Figure 19). No significant SN clusters showed a sex effect, although one cluster of 93 out of 1948 voxels was brighter in females (p=0.05). No significant clusters showed an age by sex interaction, though a negative interaction was observed in 287 out of 1948 voxels (p=0.05), indicating an increasing signal/age slope in females and a flat slope in males in the dorsal SN.

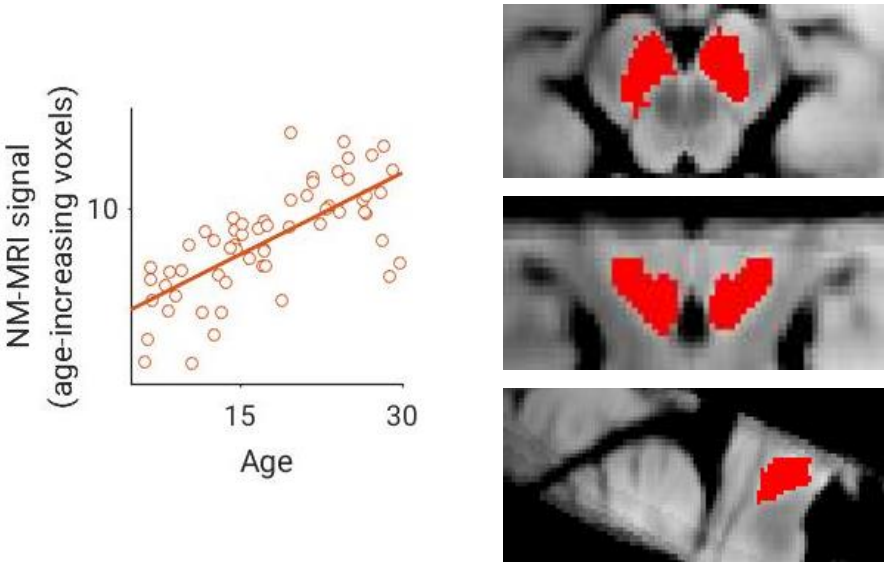

Figure 19. Voxelwise analysis of the NM-MRI signal in early life (TSE version). *The left panel shows a scatter plot of NM-MRI signal from age-increasing voxels against age. The right panels display the clusters in the SN (axial, coronal and sagittal views, descending order) where the NM-MRI signal significantly increased with age in younger participants.*

4.5 MT vs TSE comparison

Comparing the NM signal patterns between MT and TSE scans across the lifespan constitutes an important part of my second aim. One of the main goals was to identify the age at which the NM signal peak is reached for each SN voxel. To achieve this goal, different models were fitted to the lifespan NM-MRI data based on various assumptions about when the signal will peak.

The first model is the linear model; it assumes that the signal either consistently increases or decreases in each voxel with age. This assumption suggests that the NM signal either continues to increase indefinitely, beyond the lifespan, or starts at its highest point and decreases, in other words, peaking at age 0. For voxels where a linear fit was significant, but not a quadratic fit, the peak was set to age 0 or age 100 as appropriate. On the other hand, the quadratic model captures a non-linear relationship. This assumption allows the signal to peak at some point during the lifespan. To determine the age at which the NM signal peaks, the vertex formula of the quadratic equation is used. For the voxels that significantly fit the quadratic model (with a negative quadratic term), we set the age at which the NM signal peaks as the vertex of the quadratic curve, which provides the age at which the signal reaches its maximum (voxels with a positive quadratic fit were treated the same way as non-significant voxels). The voxels that did not fit any model were excluded from the analysis and not shown on Figure 20. This method allowed us to map the distribution of peak ages across voxels, offering a detailed view of how sub-regions of the SN behave over the lifespan. The SN maps showing the voxelwise analysis of NM-MRI signal peaks are shown in Figure 20.

MT and TSE scans were mostly similar with regards to the age at which the peak NM signal is reached for each voxel. The main difference, however, is a cluster of voxels in the MT scan that tends to peak very early in life and consistently decrease throughout the lifespan (shown in pink in Figure 20). The

TSE scans however, showed that the majority of voxels reach their peak signal between the ages of 40 to 50, demonstrating a non-linear relationship with age.

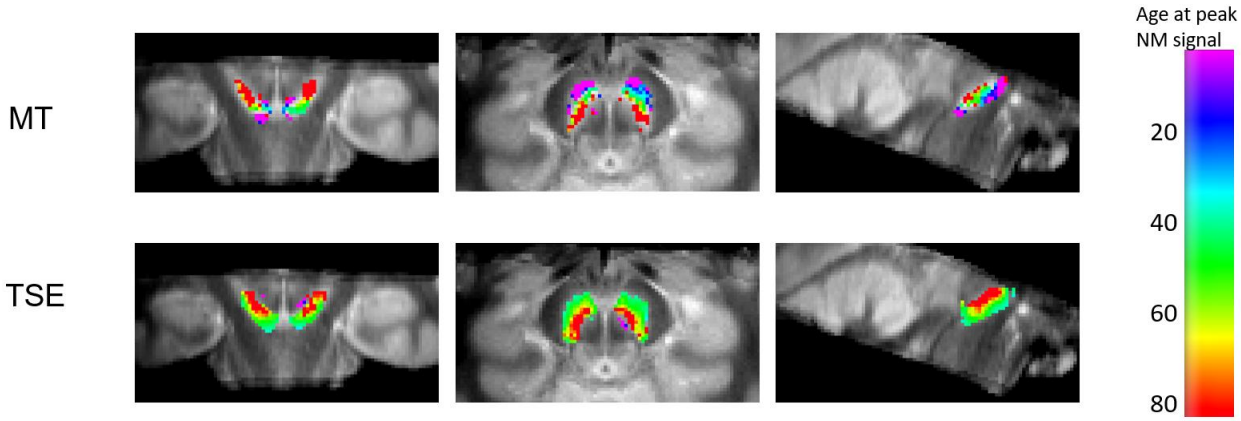

Figure 20. Voxelwise analysis of NM-MRI signal peaks in MT and TSE scans. *This figure illustrates the voxelwise analysis of the NM signal peaks in the SN across different ages, comparing MT (top row) and TSE (bottom row) scans. The color scale indicates the age at which the NM signal reaches its peak, ranging from early life (purple) to older age (red). Dorsal and middle SN were relatively similar between the 2 sequences, but ventral SN differed in that it begins to decline from birth in the MT version but increases until around age 40 in the TSE version before it declines.*

Notably, there was a strong correlation in peak ages across voxels between the two imaging methods ($r = 0.75$, $p < 10^{-99}$), indicating good agreement between the MT and TSE scans (Figure 21).

To expand the scope of our investigation of the 2 NM-MRI sequences used, we measured the level of agreement between the MT and TSE sequences using intraclass correlation coefficients (ICC). This is a statistical measure used to evaluate the consistency and reliability of NM signal in our case, while using different NM-MRI sequences, where higher values are indicative of a stronger agreement between the sequences.

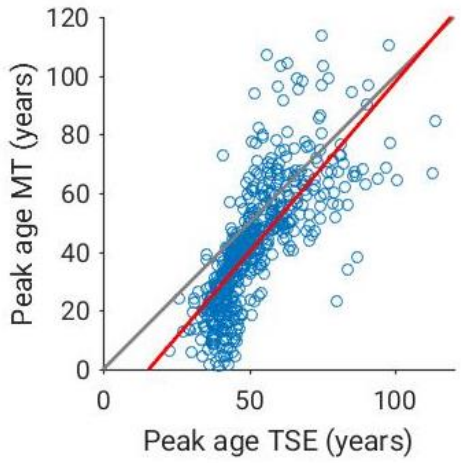

Figure 21. Correlation of peak NM signal age between MT and TSE scans. *This scatter plot shows the correlation between the peak age of NM signal in the SN as measured by MT and TSE scans. Each point represents a voxel, with the x-axis indicating the peak age in TSE scans and the y-axis indicating the peak age in MT scans. The red line represents the line of best linear fit and the gray line is the identity line (x=y). Consistent with Figure 20, there was a set of voxels showing peak age near 0 years in the MT version that had later peak age in the TSE version.*

The level of agreement on NM-MRI signal extracted from the whole SN was assessed between the TSE and MT versions. This was tested for different age bands using Intraclass correlation coefficients (ICC(3,k)). For adults aged 18-54, the ICC of whole SN signal was 0.61 and the ICC was 0.64 for adults aged 55 and older, indicating good reliability. However, in children, the ICC was only in the fair range at 0.45, suggesting that differences between the MT and TSE version are more pronounced in the case of younger populations.

Chapter 5: Investigating the link between NM signal in the SN and performance in dopamine-related cognitive tasks

This chapter shows the results generated from my third aim and seeks to investigate the relationship between NM signal in the SN and performance on the working memory task related to dopamine function.

5.1 Demographics

The sample for this aim consists of 36 participants under 18 years of age. All participants were screened to ensure they had no current psychiatric disorders or a history of lifetime psychotic disorders to simplify subsequent sections of the thesis, analyses will be constrained to use data from the MT NM-MRI sequence.

5.2 Working memory performance and NM signal

Whole SN analysis did not reveal a significant correlation with working memory performance as measured with the LSWM from the NIH Toolbox (t_{28} = 1.21, p = 0.24). However, voxelwise analysis identified a significant cluster of 289 voxels showing a positive correlation (at a height threshold of p = 0.05, cluster-size $p_{corrected}$ = 0.042), indicating localized regions within the SN where NM signal is positively associated with working memory performance (Figure 22). None of these effects were found in adults: Voxelwise analysis revealed that less than 85 out of 1948 SN voxels had some correlation with working memory scores (p > 0.05).

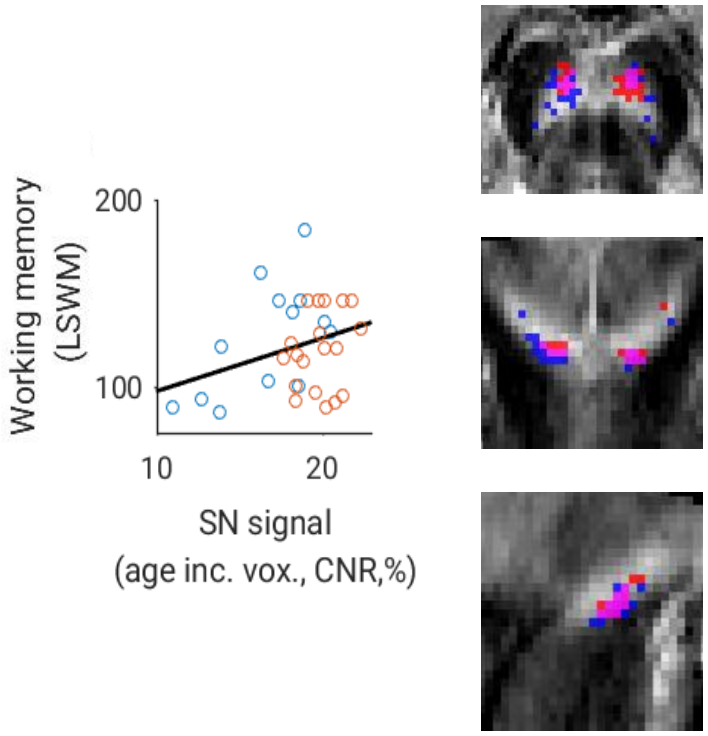

Figure 22. LSWM scores vs NM-MRI signal (MT version). *The left panel shows a scatter plot of LSWM scores against age-increasing voxels (blue: participants under 18 years old, red: participants over 18 years old).. The right panels display the working memory voxels NOT age-increasing voxels in the SN (axial, coronal and sagittal views, descending order) where the LSWM were significantly correlated with the NM-MRI signa (blue: age increasing voxels, red: WM voxels, pink: overlap).*

This analysis also showed that for children under 18 years old, the voxels where the NM-MRI signal was correlated to working memory performance overlaps well with age increasing voxels (t_{28} = 3.64, p=0.011, linear regression controlling for sex).

Chapter 6: Understanding the NM-MRI signal in the SN of children and adolescents with ADHD

This chapter shows the results for my fourth aim and examines the NM-MRI signal in the SN of children and adolescents with ADHD. It also explores the relationship between NM-MRI signal and assessing cognitive function in using the LSWM task.

6.1 NM-MRI signal in patients with ADHD

The sample for this aim consists of 53 participants under 18 years of age. Among those participants, 15 were patients diagnosed with ADHD. All healthy participants were screened to ensure they had no current psychiatric disorders or a history of lifetime psychotic disorders. The ADHD diagnosis was confirmed by medical reports from the participant's healthcare provider or by our collaborators at CHEO.

Table 6. Demographic information for HC and ADHD participants.

	Participants	n = 53
	Age range	6 - 17 years old
	HC	ADHD
Number of participants	37	15
Mean age	13.14±2.82	12.29±3.45
Males	48.37%	57.41%
Females	51.63%	42.59%

6.2 NM-MRI signal in healthy controls vs ADHD patients

We observed that the whole SN signal was significantly lower in the ADHD group compared to age-matched healthy controls (t_{49} = -2.29, p = 0.027). Voxelwise analysis revealed that 413 out of 1948 SN

voxels exhibited decreased signal in the ADHD group (at a height threshold of p = 0.05, cluster-size $p_{corrected}$ = 0.008). Most of these affected voxels were located in the left SN (Figure 23).

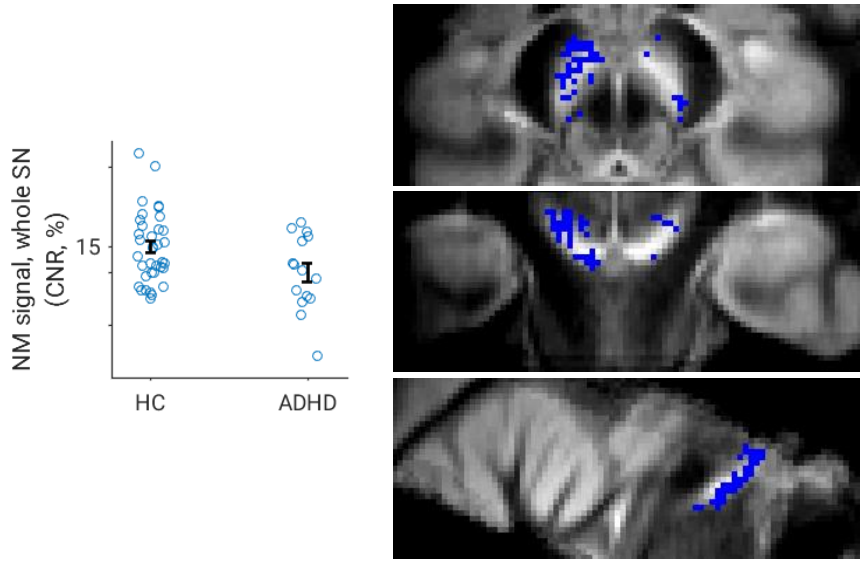

Figure 23. NM-MRI signal differences in the SN between ADHD and healthy controls. *The left panel shows a scatterplot of the NM-MRI signal in the whole SN for healthy controls and individuals with ADHD, showing a significantly lower signal in the ADHD group. The right panels display the voxels with decreased signal in the ADHD group.*

6.3 Working memory scores and NM signal in ADHD

This analysis was carried out in the ADHD group only (n = 15). Whole SN analysis did not reveal a significant correlation with LSWM performance in ADHD participants. However, lower NM-MRI signal in ADHD-associated voxels (Figure 23) was correlated with poorer working memory performance in participants with ADHD at trend level (R = 0.49, p = 0.074, n = 15, partial correlation controlling for age) (Figure 24).

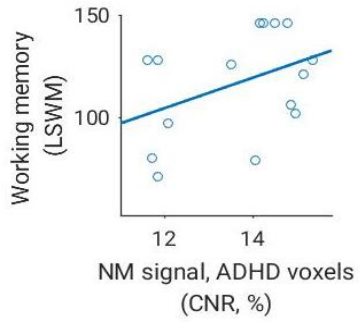

Figure 24. NM-MRI Signal in ADHD-associated voxels and working memory performance. *The scatter plot shows the relationship between NM-MRI signal in ADHD-associated voxels and LSWM scores in participants with ADHD.*

Chapter 7: Discussion

7.1 Normative values and longitudinal changes in NM-MRI signal in older adults

After completing our first aim in this project, we used a fully automated algorithm to determine the normative values for baseline NM-MRI signal and volume in the SN in a cohort of older healthy individuals with ages raging from 53 to 86 years old. We show that the values of these metrics did not change with age, suggesting that in older populations, the effect of age on the NM-MRI signal or volume is diminished. The stability that we saw in this data is important, as it indicates that age is not a factor that affects the signal in this specific age interval which supports the potential use of NM-MRI as a biomarker in clinical settings even if age norms are not explicitly integrated into the current version of the software.[159,160]

The observed data is in agreement with the general understanding that dopaminergic neurons and therefore NM content decrease with age, specifically in conditions like PD.[159] The results of this aim are valuable in showing the robustness of NM-MRI signal when used across a wide age range. The absence of significant age-related changes allows us to gain important information into the dopaminergic system integrity, while not requiring constant age adjustments. This means that over this age range, lower signal can indicate unhealthy loss of dopaminergic neurons compared to loss due to healthy aging.[26,159,161]

The data collected in this study played a pivotal role in the development of NM-101 software by Terran Biosciences, a tool that has since been FDA cleared. The normative data served two critical functions in the software's development:

The first function was determining the "normal" NM-MRI signal range in older adults. This range can be used to determine outliers where signals that fall outside of the norm can potentially identify abnormalities in the dopaminergic system, which could mean that the individual could have a psychiatric disorder or an underlying neurological condition if their NM-MRI signal is outside the expected range for their age category. With this method, early diagnosis is possible with the advantage of starting the necessary treatments needed. Note that, while this percentile information was provided in the output of the initial version of the software sent to the FDA (providing a patient with a metric, e.g. showing they are at the 55th percentile of the normative range for SN signal), this feature was removed from the final version of the software on the recommendation that a larger, more comprehensively characterized sample be used to define a more authoritative normative range.

The second function of this work was to support the development of an accurate calibration system in the NM-101 software for the signal that would be appropriate for all types of MRI scanners. MRI scanners can vary from one to another, specifically in what pertains to their software, hardware, and operational parameters, causing multiple discrepancies in NM-MRI signal measurements. This data provided a standard reference dataset to support the calibration process. This process relies on the ComBat method, similarly to the work described by Wengler and Horga.[202] By using this calibration process, any NM-MRI measurements generated from any scanner, while using the NM-101 software, can be compared for clinical and research purposes.

With the help of the newly developed software NM-101 and the normative range of values, NM-MRI imaging can now be considered an accurate diagnostic tool that can be used for clinical use, and, ultimately, to help determine any potential neurological disorders such as PD and other neurodegenerative conditions, across different patients while using any type of scanners.

In addition, since a decline in NM signal is an indication of an abnormality and potentially can lead to a clinical diagnosis, this aim highlighted the importance of determining the baseline levels of NM signal in the SN of all different age groups. [128,143] By doing so, NM-MRI can help with the development of targeted therapeutic approaches, prevention methods and treatment monitoring. NM-MRI imaging has been recently used for PD research, and these new findings in this thesis can help achieve clinical decision making for treatments and monitoring options, despite using different MRI scanners and parameters. All previously generated NM-MRI scans can be adjusted by using the ComBat method, to detect if any significant decrease in the signal and do a better and more accurate comparison and analysis of the results, as well as compare it to the healthy individuals.

Also, it is important to look at the NM signal in the different parts of the SN. As shown in Figure 9, the SN is a heterogeneous structure that has different subregions, a dorsolateral area corresponding to lateral part of SN pars compacta, a dorsomedial area corresponding to medial part of SNc and a ventral area (vSN), with different circuitry, NM accumulation levels and tissue properties.[158] This in-depth examination can be crucial in identifying specific areas within the SN that may be related to the neurodegenerative processes, or any changes associated with age.

The normative values and methodological thoroughness demonstrated in Aim 1 have a key role in promoting significant findings, particularly in the development of NM-101, an NM-MRI software created by Terran Biosciences in collaboration with Mitacs with the support of our lab (supported also by a Mitacs Accelerate Award. This was the first study to use this for-clinical-use NM-101 software to measure NM-MRI signal. Indeed, this software was still in development when this work was completed (subsequent chapters in the thesis use our standard research version of the software that allows a higher level of user control). This collaboration highlights the clinical relevance and potential impact of our work in advancing NM-MRI technology for broader clinical use. Although not directly brought up in this thesis, it is also notable that some of the data used in Aims 2-3 (TSE version) was also important in supporting the FDA

clearance of NM-101 software by providing test data to demonstrate the performance of the software's image analysis algorithm. Although this study was not designed to assess the algorithm's performance, its sensitivity in detecting SN volume changes in the expected direction over a brief time interval suggests robust performance.

Sample size was the primary limitation of this aim. It restricted our ability to divide our cohort into smaller age subgroups or based on other demographic information including sex. To allow for more precise norms, potentially facilitating the identification of neurological disorders, future research should aim at collecting a larger sample across the lifespan. However, it is promising that no significant age-related change of NM-MRI metrics was observed over this age range, supporting the usefulness of these metrics for older adults.

In addition, the normative values determined in our first aim are specific to the older population and the NM-MRI method used prior to the NM-101 software development. While we do not expect major changes when changing sequence parameters, the normative values cannot be applied universally yet to any NM-MRI acquisition. The normative values were determined using the TSE sequence, but they cannot be compared to the values obtained by other sequences such as the 2D gradient recalled echo sequence with magnetization transfer pulse (2D-GRE with MT). The TSE sequence was chosen since it is the version supported by NM-101 software because this sequence is more straightforward to implement across scanners without requiring custom sequence development that can be necessary for other sequences (e.g. for optimal use of MT sequence on Siemens scanners), thereby making it more feasible for clinical implementation.

In summary, the results acquired in the first aim allowed us to generate the standard normative values for NM-MRI signal and the volume for the SN in cognitively healthy adult people. With these values and the newly developed software NM-101 software, this NM-MRI imaging technique is a promising

diagnostic tool for clinical neuroimaging and psychiatric disorder detections. In addition, due to our findings, we were able to contribute to the FDA approval of our new software, NM-101, emphasizing the importance of our research work and the contribution of our findings to the advancement of MRI imaging technologies.

7.2 Lifespan NM dynamics: Insights from MT and TSE NM-MRI sequences

Examining the NM-MRI signal in the SN using both MT and TSE sequences throughout the lifespan provides unprecedented and detailed understanding of age-related changes of the NM signal. It also provides insights into the physical mechanisms underlying the NM-MRI contrast, which remains somewhat obscure, including the influence of NM relative to other factors that contribute to the contrast. A developmental study can provide new insights into this question since NM is minimally present at birth and increases gradually through the lifespan. These questions can be further investigated in our study by contrasting the developmental dynamics of different families of NM-MRI sequence (MT vs TSE).

Using the MT sequence, the initial linear regression analysis did not reveal any significant correlation between age the NM signal when looking at the average signal of the whole SN. This suggests that there is no clear pattern of signal change with age at the macro level of the SN.[156] It should be noted however, that this does not imply that there are no age-related changes in the NM-MRI signal in the SN, but rather highlights the need for a more granular approach to better understand NM signal variations in the SN.

This detailed approach was facilitated by voxelwise analysis, where distinct and significant clusters of voxels displayed different NM-MRI signal throughout the SN. Different subregions in the SN showed different age-related NM signal patterns, underscoring the heterogeneous nature of the SN.[25,156] This heterogeneity is key to assessing and understanding the nuanced dynamics of NM accumulation over the lifespan.[128,157,203] Clusters where the NM signal is increasing may be representing regions where the accumulation of NM continuously takes places as individuals age. More importantly, the increase that we see in the NM-MRI signal in older individuals is consistent with ongoing NM accumulation and concomitant iron deposition into older age, and supports models of NM-MRI contrast that are indeed NM-dependent.[108] On the other hand, alternative explanations that highlight the role of high free water

content in large dopamine cell bodies in driving the NM-MRI contrast independently of NM, would poorly account for the age effect on NM-MRI signal given the improbability of continued neuronal growth in advanced age.[204,205] Given the well-documented effect of iron on NM-MRI signal, a detailed examination of age-related iron dynamics within the SN could offer important data.[108,206] The persistent accumulation in certain regions in the SN could indicate ongoing neuroprotective processes in response to age-related stressors.[206] Nonetheless, the clusters showing a decrease in NM signal with age may indicate that these areas are undergoing neurodegeneration or retraction of the structure if the SN is changing shape. Indeed, there is established evidence of loss of dopaminergic neurons as, a hallmark of normal aging.[156,207]

Examination of linear relationships throughout the lifespan showed distinct patterns of NM signal changes in different regions of the SN, and exploration of non-linear relationships added another level of complexity to our understanding of NM signal dynamics. Signal in some clusters revealed a U-shaped relationship, suggesting that the NM signal in these subregions peaks at a certain age before declining. This pattern can indicate initial accumulation of the SN until a certain age, followed by a decline due to aging or pathological processes.[128]

A nearly identical cohort was examined using the TSE NM-MRI sequence. This also allowed for a comparative observation between the MT and TSE sequences. Unlike what was seen using the MT sequence, the whole SN analysis for the TSE sequence revealed a significant positive correlation between the NM signal and age, suggesting a robust NM accumulation with age when looking at the whole SN. This finding was supported by the voxelwise analysis using the TSE sequences. A large number of voxels revealed significant increases of NM signal with age, with very few exhibiting a significant decrease. This is an indicator that reductions in NM content are relatively rare and their impact on the overall age trend is not significant.

A large number of voxels exhibited a significant quadratic fit when we explored non-linear relationships in the TSE sequence analysis, indicating that the NM signal in these voxels increases to peak before decreasing. This suggests that NM accumulation follows a complex pattern, possibly due to the cumulative effects of aging and neurodegeneration.[160]

These results reveal both similarities and differences between the two versions of NM-MRI scans. Both sequences supported age-related variations in the NM signal within the SN, showing trends of NM signal changes across the lifespan. However, some differences emerged between the results of both sequences. One major difference is that when looking at the TSE version, there is only a small number of voxels exhibiting a significant decrease in NM signal throughout life, although age-related decrease may have been present in this version, if we were to restrict analysis to signal from the older population only. In the MT scan however, there are some regions with increasing signal, and other with decreasing signal, even relatively early in life, effectively neutralizing each other. This balance may have been the reason why the analysis of the average NM-MRI signal in the SN revealed that there are no age-related significant changes in NM-MRI signal when examining the MT sequence.

The detailed examination of NM signal in younger age groups provided further awareness into the developmental aspects of NM dynamics. In the MT scan, significant clusters of voxels showed increasing NM signal when looking at the younger age range, and a smaller cluster exhibited signal decrease, likely accounting for the differences observed when comparing the sequences across the full lifespan and indicating that NM accumulation is a dynamic process that starts even early life with several regional variations. On the other hand, the TSE sequences showed that most voxels exhibit a significant increase in signal, and no voxels show significant decrease in this age range. Interestingly, however, despite these noticeable differences in distribution, both MT and TSE sequences appear to be in good agreement in the younger age group, showing the same rate of increase in NM signal over time in this age range, aside from the cluster of purple voxels on Figure 20 that decline at a much earlier age according to

the MT version and may account in large part for the discrepancy between the sequences. One difference is that the curve of signal vs age starts at a higher intercept in MT sequence compared to TSE sequence, potentially indicating that NM accumulation begins at a higher level at birth (Figure 25). However, high levels of NM at birth conflict with more direct evidence and would be unlikely. It is more likely that non-NM factors that are known to also contribute to the NM-MRI contrast (i.e. large cell bodies imparting a pool of free water) are still present at birth and at this moment could reveal the portion of the contrast that is independent of NM. It may be that these non-NM factors contribute to a lesser extent to the contrast in the TSE version, lending it an intercept closer to 0 at birth. As NM signal is defined as the contrast between the SN and the reference region (Crus Cerebri) it cannot be determined from our observations that the developmental effects are entirely due to changes in the SN and not the reference region. Future work comparing the impact of employing a different reference region may also lend important insight into the discrepancies between the MT and TSE versions.

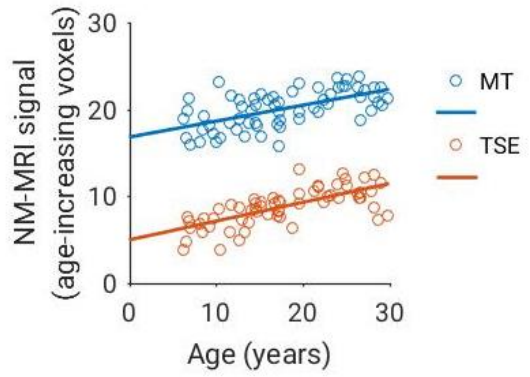

Figure 25. NM-MRI signal in age increasing voxels. Age: 6-29, n= 63 for MT, n = 60 for TSE). MT: Increase/year = 0.18 CNR units/year, signal at birth=16.9 CNR units. TSE: Increase/year = 0.18 CNR units/year, signal at birth=5.0 CNR units.

Comparing the anatomical pattern of age effects of the MT and TSE scans revealed largely similar patterns for most of the SN, for instance the dorsal SN peaks latest in life in both versions and the middle SN peaks around age 50-60 in both versions. The one region that showed a distinct pattern and could in

large part account for the differential trajectory of whole SN signal (increasing in TSE, flat in MT) is the ventral SN. The MT scans showed a cluster in the ventral SN where NM signal tended to decrease from birth, suggesting a very early peak or consistent decline in this cluster. In contrast, the TSE scans indicated that most voxels reach their peak signal between the ages of 30 and 40 in this same region, demonstrating a non-linear relationship with age. The strong correlation across SN voxels in peak ages between the two imaging methods indicates good agreement, reinforcing the reliability of these findings. One consideration that could account for these differences could be the change of the reference region, the Crus Cerebri, with age. Another consideration that could account for some of the differences between the sequences is the level of spatial correlation across voxels. This may have been higher in the TSE version as the voxel size was slightly larger, and the TSE pulses are known to blur the signal (consistent with this, we have observed that the cluster size threshold to achieve significance in permutation testing was higher in the TSE version than the MT version).[208]

The results shown in this chapter have prominent contributions towards our understanding of the dopaminergic system's aging process and underscore the importance of examining the NM signal in the SN at a finer anatomical detail. This allows to uncover changes in specific regions and is therefore crucial for developing targeted strategies and for the accurate interpretation of NM-MRI data in clinical and research settings.

The findings support the potential of NM-MRI as a tool for early diagnosis and monitoring of neurodegenerative diseases and underscore the imperative of examining the SN at higher resolution to optimize calibration of age-related confounding. Establishing the normative NM-MRI signal values across different age groups throughout the lifespan is essential for distinguishing between normal aging processes and pathological changes. This differentiation also may ultimately aid in the development of targeted pharmaceutical interventions, consistent with the promise of NM-MRI as a biomarker of response to treatments targeting the dopamine system.[198,199,202] Furthermore, the heterogeneity of the

SN is revealed by the voxelwise analysis, emphasizing the necessity of detailed anatomical examinations of this region to uncover subtle age-related changes. Focusing on the anatomy of the SN (e.g. limbic vs cognitive vs motor circuits) can allows us to increase the sensitivity and specificity of NM-MRI, contributing to better therapeutic outcomes through more personalized and targeted strategies.

7.3 NM and cognitive development in the SN

We looked specifically at the relationship between the NM signal in the SN and its effect on working memory in young participants. This confirmed that the dynamic changes we observe in NM-MRI signal during development may be relevant to important aspects of cognition.

In our initial findings, we did not observe any significant correlation between NM signal and the working memory performance when looking at the whole SN. Refining our analysis to the voxelwise level localized clusters where higher signal was correlated to better working memory performance, emphasizing the importance of analysing the SN at a higher resolution and finer anatomical level for a proper link between the functional mapping and anatomical structure of this region. Therefore, while the NM-MRI signal in the whole SN was not a predictor of WM, using voxelwise analysis showed a strong correlation between the age increasing voxels and working memory scores, in addition to a significant overlap between these voxels. Moreover, our analysis showed that the effect that was seen was mainly driven by younger participants, indicating that NM accumulation at a younger age is essential for the development of cognition.

This is consistent with our viewpoint on the SN as a heterogenous structure that is divided into separate subregions, and each subregion can have a different and specific role in cognitive function.[25] Looking closely into these subregions of the SN, each one projects to different brain areas, particularly the striatum. The striatum is subdivided into three main parts; motor striatum, cognitive striatum (also know as associative striatum), and limbic striatum (or the ventral striatum or nucleus accumbens).[30] It is well-established that the dopaminergic neurons associated with working memory project from the SN to the cognitive striatum.[30,209]

Finding this significant localized cluster of NM signal in the SN, using the MT sequence, and the established with sub-anatomical regions of the striatum and its associated cognitive function, makes this

a very promising result. It reflects the notion that NM signal accumulation with time follows a developmental trajectory where NM signal increases with age in young populations, reaching a peak at a critical point early in life. This early peak suggests the rapid development of the dopaminergic system, which is in correspondence with the fact that this period reflects the critical neurological development and cognitive growth. The lack of findings of a correlation between SN signal and working memory performance in the adult and older population suggests that this correlation may be specific to dynamic changes in the dopamine system occurring during this critical developmental period.[111,187]

The results generated in this section of the thesis show that the dynamic aspect of the dopaminergic system is at its peak during the periods where the brain is still in development and then stabilizes after the brain maturation is reached. This suggests that the NM signal and the cognitive function are not static but mainly evolve across the lifespan during the early stages of life. With these findings, we have a better understanding of the relationship between the dopaminergic system and the cognitive development.

7.4 NM as a biomarker in ADHD

The findings of this part of my thesis reveal important neurobiological mechanisms of childhood ADHD by means of NM dynamics in the SN, when examining the MT sequence. Signal differences in NM-MRI between participants with ADHD and the control group underscores the role of the dopaminergic system in the manifestation of ADHD symptoms.

The main observation is the significantly lower NM-MRI signal observed in the SN of ADHD participants compared to healthy controls. This reduction reflects diminished NM content, reflecting a lower density or reduced activity of dopaminergic neurons within the SN. These results are consistent with current evidence found in the literature, where abnormal dopamine transmission was found in the striatum and prefrontal cortex, brain regions associated with attention and impulse control.[210–212] PET studies in adults showed regional hypoactivity of attention and motor control areas.[210] Moreover, fMRI studies in adolescents diagnosed with ADHD showed significantly altered resting-state signal in different brain regions involved in cognitive control compared to their healthy peers.[211] Given that NM accumulation is indicative of a healthy dopaminergic function in the brain, our result points to an underlying dysfunction in the dopaminergic system in the ADHD group, possibly leading to the most common symptoms of ADHD including attention regulation, impulse control and other cognitive function.[114,195,197]

Another notable observation is that the majority of the voxels affected by this decrease are localized in the left SN. This laterization, revealed by voxelwise analysis, is particularly interesting, since numerous studies underscore the left hemisphere's established role in executive function and motor control, areas affected in individuals with ADHD.[213,214] This developmental specificity suggests that the maturation of the dopaminergic system and impact on dopamine-related functions is particularly dynamic in children and adolescents.

The promise of these findings extends beyond boosting our understanding of ADHD. The significant correlation between NM-MRI signal reductions and ADHD symptoms suggests that NM could serve as a valuable biomarker for clinical conditions like ADHD. In addition, although not significant, but the correlation between working memory performance and NM-MRI signal in ADHD participants is promising given that the results were obtained using an underpowered sample. Demonstrating that NM-MRI can reliably detect neurobiological changes associated with ADHD opens new avenues for using this imaging technique in clinical settings, potentially allowing for earlier and more accurate diagnosis, as well as monitoring treatment efficacy over time.

Chapter 8: Limitations, future directions, and conclusion

8.1 Limitations

A primary limitation of the first aim is sample size, restricting our ability to divide the sample into smaller age subgroups. Another limitation is that no other demographic factors than age were examined, and their effect on the signal was not studied. Also, it would have been more ideal to have similar time gaps between baseline and follow-up scans. This would allow for more precise norms, potentially narrowing their range and facilitating the identification of individuals at risk for neurodegenerative or psychiatric illnesses.

A potential limitation of the second aim is the reliance on different NM-MRI sequences (MT and TSE) and their inherent variations. The TSE sequence predominantly shows increasing signal, which could lead to an oversimplified view of NM accumulation, unlike the MT sequence, that shows different patterns. Another limitation could be attributed to the reference region used, the Crus Cerebri, and the lack of knowledge about the change of this structure with age. Other reference regions could be explored as well, including the periaqueductal grey or the red nucleus.[143,215]

Relying on measuring cognitive function using only one test could be the limitation of the third aim. A large number of validated cognitive tests are available to use, and other options should have been explored to further confirm our findings.

In the fourth aim, our ADHD sample consisted of patients who were at different stages of their treatment, potentially affecting the outcome of our testing. A larger sample size is needed, ideally in the first stages of ADHD treatment or severity, which would reflect a better understanding of how NM signal changes in ADHD. For instance, exposure to psychostimulant medication could conceivably impact the NM-MRI signal, potentially confounding our ability to see the association with ADHD and we were not

able to adequately assess this. Also, children with ADHD could be more prone to motion in the scanner which could impact our NM-MRI metrics.

8.2 Future directions

In general, subsequent research should aim at expanding sample size across different age groups in all the aims of this research. In addition, more demographic factors should be considered while doing different analyses. Additionally, longitudinal studies are needed to better understand how NM development throughout life, in addition to better understand cognitive function. In fact, longitudinal data for NMLife is already being collected at the Royal, and we hope to finish data collection by December 2025. Testing changes in the reference region, the Crus Cerebri, could increase our understanding of the changes of signal in the SN; it could be a contributor for some of the changes we see in our results. Finally, advancing the technical aspects of NM-MRI, such as improving sequence sensitivity and specificity, and understanding the physical and biological mechanisms that affect the signal in the two sequences will be key to maximizing its clinical utility.

8.3 Conclusion

This thesis has provided comprehensive insights into the dynamics of NM within the SN across various stages of life, from childhood to old age, and its potential role as a biomarker for neurodegenerative and neurodevelopmental conditions.

The first major finding of this thesis was the establishment of normative values for the NM-MRI metrics in the SN of older adults. The work showed a relatively stable signal in late life, providing important understanding for distinguishing between normal aging and changes caused by pathological conditions.

Upon further examining NM dynamics across the lifespan, using two different NM-MRI sequences, we revealed that it is not only crucial to look at the average NM signal in the SN, but that it is more beneficial to study how the signal changes in different voxels of the SN through voxelwise analysis. We also showed that although some key differences are present between the MT and TSE versions, both showed some consistent trends in signal variations.

Investigating the relationship between cognitive function and NM signal in the younger age range provided additional data on the dynamic aspect of the development of the dopaminergic system in early life. The significant finding emphasizes the role of NM not only as a biomarker to monitor neurodegenerative or psychiatric conditions, but also as a valuable tool to monitor changes in healthy individuals and better understand the dynamics and effects of the dopaminergic system.

This study also explored the ability of NM-MRI to detect NM changes in children adolescents with ADHD. This further highlights the potential use of NM as a biomarker for this disorder, offering new avenues for early diagnosis and treatment monitoring.

In conclusion, this thesis has not only expanded our understanding of NM dynamics across the lifespan but also demonstrated the utility of NM-MRI as a powerful tool for studying the dopaminergic

system in both health and disease. The findings underscore the potential of NM-MRI to serve as a biomarker for various clinical conditions, paving the way for more personalized and targeted therapeutic strategies in the future.

Chapter 9: References

1. Juárez Olguín, H., Calderón Guzmán, D., Hernández García, E. & Barragán Mejía, G. The Role of Dopamine and Its Dysfunction as a Consequence of Oxidative Stress. *Oxid. Med. Cell. Longev.* **2016**, 9730467 (2016).
2. Catecholamine Synthesis - an overview | ScienceDirect Topics. https://www.sciencedirect.com/topics/medicine-and-dentistry/catecholamine-synthesis.
3. Daubner, S. C., Le, T. & Wang, S. Tyrosine Hydroxylase and Regulation of Dopamine Synthesis. *Arch. Biochem. Biophys.* **508**, 1–12 (2011).
4. Meiser, J., Weindl, D. & Hiller, K. Complexity of dopamine metabolism. *Cell Commun. Signal. CCS* **11**, 34 (2013).
5. Amino Acid Decarboxylase - an overview | ScienceDirect Topics. https://www.sciencedirect.com/topics/medicine-and-dentistry/amino-acid-decarboxylase.
6. Carboxylyase - an overview | ScienceDirect Topics. https://www.sciencedirect.com/topics/medicine-and-dentistry/carboxylyase.
7. German, C. L., Baladi, M. G., McFadden, L. M., Hanson, G. R. & Fleckenstein, A. E. Regulation of the Dopamine and Vesicular Monoamine Transporters: Pharmacological Targets and Implications for Disease. *Pharmacol. Rev.* **67**, 1005–1024 (2015).
8. Wimalasena, K. Vesicular Monoamine Transporters: Structure-Function, Pharmacology, and Medicinal Chemistry. *Med. Res. Rev.* **31**, 483–519 (2011).
9. Klein, M. O. *et al.* Dopamine: Functions, Signaling, and Association with Neurological Diseases. *Cell. Mol. Neurobiol.* **39**, 31–59 (2019).
10. Tripathi, A., Appavu, R. & Kethar, J. The Age of the Meta-Doctor: Diagnosing Parkinson's Disease with Artificial Intelligence and Speech. *J. Stud. Res.* **12**, (2023).

11. Harris, K. D., Weiss, M. & Zahavi, A. Why are neurotransmitters neurotoxic? An evolutionary perspective. *F1000Research* **3**, 179 (2014).
12. Cai, J. & Tong, Q. Anatomy and Function of Ventral Tegmental Area Glutamate Neurons. *Front. Neural Circuits* **16**, 867053 (2022).
13. Sonne, J., Reddy, V. & Beato, M. R. Neuroanatomy, Substantia Nigra. in *StatPearls* (StatPearls Publishing, Treasure Island (FL), 2020).
14. Luo, S. X. & Huang, E. J. Dopaminergic Neurons and Brain Reward Pathways. *Am. J. Pathol.* **186**, 478–488 (2016).
15. Bamford, I. J. & Bamford, N. S. The Striatum's Role in Executing Rational and Irrational Economic Behaviors. *Neurosci. Rev. J. Bringing Neurobiol. Neurol. Psychiatry* **25**, 475–490 (2019).
16. Martel, J. C. & Gatti McArthur, S. Dopamine Receptor Subtypes, Physiology and Pharmacology: New Ligands and Concepts in Schizophrenia. *Front. Pharmacol.* **11**, (2020).
17. Tritsch, N. X. & Sabatini, B. L. Dopaminergic modulation of synaptic transmission in cortex and striatum. *Neuron* **76**, 33–50 (2012).
18. Reneman, L., van der Pluijm, M., Schrantee, A. & Giessen, E. Imaging of the dopamine system with focus on pharmacological MRI and neuromelanin imaging. *Eur. J. Radiol.* **140**, 109752 (2021).
19. Mishra, A., Singh, S. & Shukla, S. Physiological and Functional Basis of Dopamine Receptors and Their Role in Neurogenesis: Possible Implication for Parkinson's disease. *J. Exp. Neurosci.* **12**, (2018).
20. Rocha, G. S. *et al.* Basal ganglia for beginners: the basic concepts you need to know and their role in movement control. *Front. Syst. Neurosci.* **17**, 1242929 (2023).

21. Weinstein, J. J. *et al.* Pathway-specific dopamine abnormalities in schizophrenia. *Biol. Psychiatry* **81**, 31–42 (2017).
22. Luvsannyam, E. *et al.* Neurobiology of Schizophrenia: A Comprehensive Review. *Cureus* **14**, e23959.
23. Tyng, C. M., Amin, H. U., Saad, M. N. M. & Malik, A. S. The Influences of Emotion on Learning and Memory. *Front. Psychol.* **8**, 1454 (2017).
24. Zhai, S., Shen, W., Graves, S. M. & Surmeier, D. J. Dopaminergic modulation of striatal function and Parkinson's disease. *J. Neural Transm. Vienna Austria 1996* **126**, 411 (2019).
25. Zhang, Y., Larcher, K. M.-H., Misic, B. & Dagher, A. Anatomical and functional organization of the human substantia nigra and its connections. *eLife* **6**, e26653 (2017).
26. Ramesh, S. & Arachchige, A. S. P. M. Depletion of dopamine in Parkinson's disease and relevant therapeutic options: A review of the literature. *AIMS Neurosci.* **10**, 200–231 (2023).
27. van de Giessen, E. *et al.* Deficits in striatal dopamine release in cannabis dependence. *Mol. Psychiatry* **22**, 68–75 (2017).
28. Lanciego, J. L., Luquin, N. & Obeso, J. A. Functional Neuroanatomy of the Basal Ganglia. *Cold Spring Harb. Perspect. Med.* **2**, a009621 (2012).
29. Gerfen, C. R. Segregation of D1 and D2 dopamine receptors in the striatal direct and indirect pathways: An historical perspective. *Front. Synaptic Neurosci.* **14**, 1002960 (2023).
30. van den Bosch, R. *et al.* Evidence for absence of links between striatal dopamine synthesis capacity and working memory capacity, spontaneous eye-blink rate, and trait impulsivity. *eLife* **12**, e83161.
31. Tessitore, A., Cirillo, M. & De Micco, R. Functional Connectivity Signatures of Parkinson's Disease. *J. Park. Dis.* **9**, 637–652.

32. Kouli, A., Torsney, K. M. & Kuan, W.-L. Parkinson's Disease: Etiology, Neuropathology, and Pathogenesis. in *Parkinson's Disease: Pathogenesis and Clinical Aspects* (eds. Stoker, T. B. & Greenland, J. C.) (Codon Publications, Brisbane (AU), 2018).
33. Kehagia, A. A., Barker, R. A. & Robbins, T. W. Cognitive Impairment in Parkinson's Disease: The Dual Syndrome Hypothesis. *Neurodegener. Dis.* **11**, 79–92 (2012).
34. Lewitt, P. A. Levodopa for the treatment of Parkinson's disease. *N. Engl. J. Med.* **359**, 2468–2476 (2008).
35. Cowan, N. Working Memory Underpins Cognitive Development, Learning, and Education. *Educ. Psychol. Rev.* **26**, 197–223 (2014).
36. Li, W. *et al.* Longitudinal functional connectivity changes related to dopaminergic decline in Parkinson's disease. *NeuroImage Clin.* **28**, 102409 (2020).
37. Williams, G. V. & Goldman-Rakic, P. S. Modulation of memory fields by dopamine Dl receptors in prefrontal cortex. *Nature* **376**, 572–575 (1995).
38. Arnsten, A. F. T. The Neurobiology of Thought: The Groundbreaking Discoveries of Patricia Goldman-Rakic 1937–2003. *Cereb. Cortex N. Y. NY* **23**, 2269–2281 (2013).
39. Goldman-Rakic, P. S. Circuitry of the frontal association cortex and its relevance to dementia. *Arch. Gerontol. Geriatr.* **6**, 299–309 (1987).
40. Goldman-Rakic, P. S. Cellular basis of working memory. *Neuron* **14**, 477–485 (1995).
41. Puig, M. V., Rose, J., Schmidt, R. & Freund, N. Dopamine modulation of learning and memory in the prefrontal cortex: insights from studies in primates, rodents, and birds. *Front. Neural Circuits* **8**, 93 (2014).
42. Grospe, G. M., Baker, P. M. & Ragozzino, M. E. Cognitive Flexibility Deficits Following 6-OHDA Lesions of the Rat Dorsomedial Striatum. *Neuroscience* **374**, 80–90 (2018).

43. Ardayfio, P., Youn-Hwang, D., Leung, A., Moon, J. & Kim, K.-S. Impaired Learning and Memory in Pitx3 Deficient aphakia mice: A Genetic Model for Striatum-Dependent Cognitive Symptoms in Parkinson's Disease. *Neurobiol. Dis.* **31**, 406–412 (2008).
44. Fallon, S. J., Zokaei, N., Norbury, A., Manohar, S. G. & Husain, M. Dopamine Alters the Fidelity of Working Memory Representations according to Attentional Demands. *J. Cogn. Neurosci.* **29**, 728–738 (2017).
45. Homberg, J. R. *et al.* The role of the dopamine D1 receptor in social cognition: studies using a novel genetic rat model-. *Dis. Model. Mech.* **9**, 1147–1158 (2016).
46. Chen, A. P., Chen, L., Kim, T. A. & Xiong, Q. Integrating the Roles of Midbrain Dopamine Circuits in Behavior and Neuropsychiatric Disease. *Biomedicines* **9**, 647 (2021).
47. Paloyelis, Y., Mehta, M. A., Kuntsi, J. & Asherson, P. Functional magnetic resonance imaging in attention deficit hyperactivity disorder (ADHD): a systematic literature review. *Expert Rev. Neurother.* **7**, 1337–1356 (2007).
48. Miller, D. J., Derefinko, K. J., Lynam, D. R., Milich, R. & Fillmore, M. T. Impulsivity and Attention Deficit-Hyperactivity Disorder: Subtype Classification Using the UPPS Impulsive Behavior Scale. *J. Psychopathol. Behav. Assess.* **32**, 323–332 (2010).
49. Klanker, M., Feenstra, M. & Denys, D. Dopaminergic control of cognitive flexibility in humans and animals. *Front. Neurosci.* **7**, 201 (2013).
50. Drechsler, R. *et al.* ADHD: Current Concepts and Treatments in Children and Adolescents. *Neuropediatrics* **51**, 315–335 (2020).
51. Gardner, E. L. Introduction: Addiction and Brain Reward and Anti-Reward Pathways. *Adv. Psychosom. Med.* **30**, 22–60 (2011).
52. Bromberg-Martin, E. S., Matsumoto, M. & Hikosaka, O. Dopamine in motivational control: rewarding, aversive, and alerting. *Neuron* **68**, 815–834 (2010).

53. Westbrook, A. & Braver, T. S. Dopamine does double duty in motivating cognitive effort. *Neuron* **89**, 695–710 (2016).
54. Cassidy, C. M. *et al.* Evidence for Dopamine Abnormalities in the Substantia Nigra in Cocaine Addiction Revealed by Neuromelanin-Sensitive MRI. *Am. J. Psychiatry* **177**, 1038–1047 (2020).
55. Schultz, W. Dopamine reward prediction error coding. *Dialogues Clin. Neurosci.* **18**, 23–32 (2016).
56. Schultz, W., Dayan, P. & Montague, P. R. A neural substrate of prediction and reward. *Science* **275**, 1593–1599 (1997).
57. Keiflin, R. & Janak, P. H. Dopamine prediction errors in reward learning and addiction: from theory to neural circuitry. *Neuron* **88**, 247–263 (2015).
58. Carlsson, A., Lindqvist, M., Magnusson, T. & Waldeck, B. On the presence of 3-hydroxytyramine in brain. *Science* **127**, 471 (1958).
59. Carlsson, A., Lindqvist, M. & Magnusson, T. 3,4-Dihydroxyphenylalanine and 5-hydroxytryptophan as reserpine antagonists. *Nature* **180**, 1200 (1957).
60. Howes, O. D. & Kapur, S. The dopamine hypothesis of schizophrenia: version III--the final common pathway. *Schizophr. Bull.* **35**, 549–562 (2009).
61. The Nobel Prize in Physiology or Medicine 2000. *NobelPrize.org* https://www.nobelprize.org/prizes/medicine/2000/7621-the-nobel-prize-in-physiology-or-medicine-2000/.
62. Hornykiewicz, O. Dopamine (3-hydroxytyramine) and brain function. *Pharmacol. Rev.* **18**, 925–964 (1966).
63. Gandhi, K. R. & Saadabadi, A. Levodopa (L-Dopa). in *StatPearls* (StatPearls Publishing, Treasure Island (FL), 2024).

64. Dahoun, T. *et al*. The relationship between childhood trauma, dopamine release and dexamphetamine-induced positive psychotic symptoms: a [11C]-(+)-PHNO PET study. *Transl. Psychiatry* **9**, 1–12 (2019).
65. Lamelle, M. & Abi-Dargham, A. Dopamine in the history of the schizophrenic brain: recent contributions of brain-imaging studies. *Dialogues Clin. Neurosci.* **2**, 359–372 (2000).
66. Shen, L.-H., Liao, M.-H. & Tseng, Y.-C. Recent Advances in Imaging of Dopaminergic Neurons for Evaluation of Neuropsychiatric Disorders. *J. Biomed. Biotechnol.* **2012**, 259349 (2012).
67. Laruelle, M. & Abi-Dargham, A. Dopamine as the wind of the psychotic fire: new evidence from brain imaging studies. *J. Psychopharmacol. (Oxf.)* **13**, 358–371 (1999).
68. Halliday, G. M., Holton, J. L., Revesz, T. & Dickson, D. W. Neuropathology underlying clinical variability in patients with synucleinopathies. *Acta Neuropathol. (Berl.)* **122**, 187–204 (2011).
69. Halliday, G. M., Leverenz, J. B., Schneider, J. S. & Adler, C. H. The Neurobiological Basis of Cognitive Impairment in Parkinson'S Disease. *Mov. Disord. Off. J. Mov. Disord. Soc.* **29**, 634–650 (2014).
70. Tan, Y.-Y., Jenner, P. & Chen, S.-D. Monoamine Oxidase-B Inhibitors for the Treatment of Parkinson's Disease: Past, Present, and Future. *J. Park. Dis.* **12**, 477–493.
71. Hoops, D. & Flores, C. Making Dopamine Connections in Adolescence. *Trends Neurosci.* **40**, 709–719 (2017).
72. Niederkofler, V., Asher, T. E. & Dymecki, S. M. Functional Interplay between Dopaminergic and Serotonergic Neuronal Systems during Development and Adulthood. *ACS Chem. Neurosci.* **6**, 1055–1070 (2015).
73. Milbocker, K. *et al.* Glia-Driven Brain Circuit Refinement Is Altered by Early-Life Adversity: Behavioral Outcomes. *Front. Behav. Neurosci.* **15**, (2021).

74. Stiles, J. & Jernigan, T. L. The Basics of Brain Development. *Neuropsychol. Rev.* **20**, 327–348 (2010).
75. Cellular Programming and Reprogramming: Sculpting Cell Fate for the Production of Dopamine Neurons for Cell Therapy - PMC. https://www.ncbi.nlm.nih.gov/pmc/articles/PMC3441013/.
76. Hynes, M. & Rosenthal, A. Specification of dopaminergic and serotonergic neurons in the vertebrate CNS. *Curr. Opin. Neurobiol.* **9**, 26–36 (1999).
77. van Dyck, L. I. & Morrow, E. M. Genetic control of postnatal human brain growth. *Curr. Opin. Neurol.* **30**, 114–124 (2017).
78. Arain, M. *et al.* Maturation of the adolescent brain. *Neuropsychiatr. Dis. Treat.* **9**, 449–461 (2013).
79. Reynolds, R. *et al.* A systematic review of chronic disease management interventions in primary care. *BMC Fam. Pract.* **19**, 11 (2018).
80. Adolescence as a neurobiological critical period for the development of higher-order cognition - PMC. https://www.ncbi.nlm.nih.gov/pmc/articles/PMC6526538/.
81. National Academies of Sciences, E. *et al.* Adolescent Development. in *The Promise of Adolescence: Realizing Opportunity for All Youth* (National Academies Press (US), 2019).
82. Boyer, N. P. & Gupton, S. L. Revisiting Netrin-1: One Who Guides (Axons). *Front. Cell. Neurosci.* **12**, (2018).
83. Vosberg, D. E., Leyton, M. & Flores, C. The Netrin-1/DCC guidance system: dopamine pathway maturation and psychiatric disorders emerging in adolescence. *Mol. Psychiatry* **25**, 297–307 (2020).
84. Reynolds, L. M. *et al.* Amphetamine disrupts dopamine axon growth in adolescence by a sex-specific mechanism in mice. *Nat. Commun.* **14**, 4035 (2023).

85. Sakai, J. Core Concept: How synaptic pruning shapes neural wiring during development and, possibly, in disease. *Proc. Natl. Acad. Sci. U. S. A.* **117**, 16096–16099 (2020).
86. Mechanisms governing activity-dependent synaptic pruning in the mammalian CNS - PMC. https://www.ncbi.nlm.nih.gov/pmc/articles/PMC8541743/.
87. Pruning recurrent neural networks replicates adolescent changes in working memory and reinforcement learning | PNAS. https://www.pnas.org/doi/10.1073/pnas.2121331119.
88. Evrard, M. R., Li, M., Shen, H. & Smith, S. S. Preventing adolescent synaptic pruning in mouse prelimbic cortex via local knockdown of α4βδ GABAA receptors increases anxiety response in adulthood. *Sci. Rep.* **11**, 21059 (2021).
89. Myelin development in cerebral gray and white matter during adolescence and late childhood - PMC. https://pmc.ncbi.nlm.nih.gov/articles/PMC8214999/.
90. McDougall, S. *et al.* Myelination of Axons Corresponds with Faster Transmission Speed in the Prefrontal Cortex of Developing Male Rats. *eNeuro* **5**, ENEURO.0203-18.2018 (2018).
91. Myelin, Membrane | Learn Science at Scitable. https://www.nature.com/scitable/topicpage/myelin-a-specialized-membrane-for-cell-communication-14367205/.
92. Friedman, N. P. & Robbins, T. W. The role of prefrontal cortex in cognitive control and executive function. *Neuropsychopharmacology* **47**, 72–89 (2022).
93. Wahlstrom, D., Collins, P., White, T. & Luciana, M. Developmental Changes in Dopamine Neurotransmission in Adolescence: Behavioral Implications and Issues in Assessment. *Brain Cogn.* **72**, 146 (2010).
94. Corrigan, N. M. *et al.* Myelin development in cerebral gray and white matter during adolescence and late childhood. *NeuroImage* **227**, 117678 (2021).

95. Squeglia, L. M., Jacobus, J. & Tapert, S. F. The Influence of Substance Use on Adolescent Brain Development. *Clin. EEG Neurosci. Off. J. EEG Clin. Neurosci. Soc. ENCS* **40**, 31–38 (2009).

96. Schweinsburg, A. D., McQueeny, T., Nagel, B. J., Eyler, L. T. & Tapert, S. F. A preliminary study of functional magnetic resonance imaging response during verbal encoding among adolescent binge drinkers. *Alcohol* **44**, 111–117 (2010).

97. Mason, M., Mennis, J., Russell, M., Moore, M. & Brown, A. Adolescent Depression and Substance Use: The Protective Role of Prosocial Peer Behavior. *J. Abnorm. Child Psychol.* **47**, 1065–1074 (2019).

98. Toftdahl, N. G., Nordentoft, M. & Hjorthøj, C. Prevalence of substance use disorders in psychiatric patients: a nationwide Danish population-based study. *Soc. Psychiatry Psychiatr. Epidemiol.* **51**, 129–140 (2016).

99. Hamidullah, S., Thorpe, H. H. A., Frie, J. A., Mccurdy, R. D. & Khokhar, J. Y. Adolescent Substance Use and the Brain: Behavioral, Cognitive and Neuroimaging Correlates. *Front. Hum. Neurosci.* **14**, (2020).

100. Reichelt, A. C. Adolescent Maturational Transitions in the Prefrontal Cortex and Dopamine Signaling as a Risk Factor for the Development of Obesity and High Fat/High Sugar Diet Induced Cognitive Deficits. *Front. Behav. Neurosci.* **10**, 189 (2016).

101. Hammond, C. J., Mayes, L. C. & Potenza, M. N. Neurobiology of Adolescent Substance Use and Addictive Behaviors: Prevention and Treatment Implications. *Adolesc. Med. State Art Rev.* **25**, 15–32 (2014).

102. Steinberg, L. A Social Neuroscience Perspective on Adolescent Risk-Taking. *Dev. Rev. DR* **28**, 78–106 (2008).

103. Lourenco, F. & Casey, B. Adjusting Behavior to Changing Environmental Demands with Development. *Neurosci. Biobehav. Rev.* **37**, 10.1016/j.neubiorev.2013.03.003 (2013).

104. Price, R. B. & Duman, R. Neuroplasticity in cognitive and psychological mechanisms of depression: An integrative model. *Mol. Psychiatry* **25**, 530–543 (2020).

105. Taylor, W. D. *et al.* Influences of Dopaminergic System Dysfunction on Late-Life Depression. *Mol. Psychiatry* **27**, 180–191 (2022).

106. Seidler, R. D. *et al.* Motor Control and Aging: Links to Age-Related Brain Structural, Functional, and Biochemical Effects. *Neurosci. Biobehav. Rev.* **34**, 721–733 (2010).

107. Cloak, N., Schoo, C. & Al Khalili, Y. Behavioral and Psychological Symptoms in Dementia. in *StatPearls* (StatPearls Publishing, Treasure Island (FL), 2024).

108. Zucca, F. A. *et al.* Interactions of iron, dopamine and neuromelanin pathways in brain aging and Parkinson's disease. *Prog. Neurobiol.* **155**, 96–119 (2017).

109. Mahul-Mellier, A.-L. *et al.* The process of Lewy body formation, rather than simply α-synuclein fibrillization, is one of the major drivers of neurodegeneration. *Proc. Natl. Acad. Sci.* **117**, 4971–4982 (2020).

110. Zwaigenbaum, L. *et al.* Early Identification and Interventions for Autism Spectrum Disorder: Executive Summary. *Pediatrics* **136**, S1–S9 (2015).

111. Areal, L. B. & Blakely, R. D. Neurobehavioral Changes Arising from Early Life Dopamine Signaling Perturbations. *Neurochem. Int.* **137**, 104747 (2020).

112. Arnsten, A. F. T. The Emerging Neurobiology of Attention Deficit Hyperactivity Disorder: The Key Role of the Prefrontal Association Cortex. *J. Pediatr.* **154**, I-S43 (2009).

113. Spencer, T. J. *et al.* Further Evidence of Dopamine Transporter Receptor Dysregulation in ADHD: A Controlled PET Imaging Study Using Altropane. *Biol. Psychiatry* **62**, 1059–1061 (2007).

114. Volkow, N. D. *et al.* Evaluating dopamine reward pathway in ADHD: clinical implications. *JAMA* **302**, 1084–1091 (2009).

115. Spencer, T. J. *et al.* Effect of psychostimulants on brain structure and function in ADHD: a qualitative literature review of magnetic resonance imaging-based neuroimaging studies. *J. Clin. Psychiatry* **74**, 902–917 (2013).

116. Pavăl, D. A Dopamine Hypothesis of Autism Spectrum Disorder. *Dev. Neurosci.* **39**, 355–360 (2017).

117. Jiang, C.-C. *et al.* Signalling pathways in autism spectrum disorder: mechanisms and therapeutic implications. *Signal Transduct. Target. Ther.* **7**, 1–36 (2022).

118. Rothwell, P. E. *et al.* Autism-associated neuroligin-3 mutations commonly impair striatal circuits to boost repetitive behaviors. *Cell* **158**, 198–212 (2014).

119. Vissers, M. E., X Cohen, M. & Geurts, H. M. Brain connectivity and high functioning autism: A promising path of research that needs refined models, methodological convergence, and stronger behavioral links. *Neurosci. Biobehav. Rev.* **36**, 604–625 (2012).

120. Wegiel, J. *et al.* Brain-region–specific alterations of the trajectories of neuronal volume growth throughout the lifespan in autism. *Acta Neuropathol. Commun.* **2**, 28 (2014).

121. Pavăl, D. & Miclutia, I. The Dopamine Hypothesis of Autism Spectrum Disorder Revisited: Current Status and Future Prospects. *Dev. Neurosci.* **43**, 1–11 (2021).

122. Theoharides, T. C. & Zhang, B. Neuro-inflammation, blood-brain barrier, seizures and autism. *J. Neuroinflammation* **8**, 168 (2011).

123. Lu, X. *et al.* Developmental Dopaminergic Signaling Modulates Neural Circuit Formation and Contributes to Autism Spectrum Disorder–Related Phenotypes. *Am. J. Pathol.* **194**, 1062–1077 (2024).

124. Buse, J., Schoenefeld, K., Münchau, A. & Roessner, V. Neuromodulation in Tourette syndrome: Dopamine and beyond. *Neurosci. Biobehav. Rev.* **37**, 1069–1084 (2013).

125. Peters, R. Ageing and the brain. *Postgrad. Med. J.* **82**, 84–88 (2006).

126. Berry, A. S. *et al*. Aging Affects Dopaminergic Neural Mechanisms of Cognitive Flexibility. *J. Neurosci*. **36**, 12559–12569 (2016).

127. Coleman, C. & Martin, I. Unraveling Parkinson's Disease Neurodegeneration: Does Aging Hold the Clues? *J. Park. Dis*. **12**, 2321–2338.

128. Xing, Y., Sapuan, A., Dineen, R. A. & Auer, D. P. Life span pigmentation changes of the substantia nigra detected by neuromelanin-sensitive MRI. *Mov. Disord. Off. J. Mov. Disord. Soc*. **33**, 1792–1799 (2018).

129. Di Lorenzo Alho, A. T. *et al*. Three-dimensional and stereological characterization of the human substantia nigra during aging. *Brain Struct. Funct*. **221**, 3393–3403 (2016).

130. Chatterjee, D. & Gerlai, R. High precision liquid chromatography analysis of dopaminergic and serotoninergic responses to acute alcohol exposure in zebrafish. *Behav. Brain Res*. **200**, 208–213 (2009).

131. Church, W. H. Column Chromatography Analysis of Brain Tissue: An Advanced Laboratory Exercise for Neuroscience Majors. *J. Undergrad. Neurosci. Educ*. **3**, A36–A41 (2005).

132. Chefer, V. I., Thompson, A. C., Zapata, A. & Shippenberg, T. S. Overview of Brain Microdialysis. *Curr. Protoc. Neurosci. Editor. Board Jacqueline N Crawley Al* **CHAPTER**, Unit7.1 (2009).

133. Verger, A., Grimaldi, S., Ribeiro, M., Frismand, S. & Guedj, E. Single Photon Emission Computed Tomography/Positron Emission Tomography Molecular Imaging for Parkinsonism: A Fast-Developing Field. *Ann. Neurol*. **90**, 711–719 (2021).

134. Anand, S., Singh, H. & Dash, A. Clinical Applications of PET and PET-CT. *Med. J. Armed Forces India* **65**, 353–358 (2009).

135. Shippenberg, T. S. & Thompson, A. C. Overview of Microdialysis. *Curr. Protoc. Neurosci. Editor. Board Jacqueline N Crawley Al* **CHAPTER**, Unit7.1 (2001).

136. Darvesh, A. S. *et al.* In vivo brain microdialysis: advances in neuropsychopharmacology and drug discovery. *Expert Opin. Drug Discov.* **6**, 109–127 (2011).

137. Tjahjono, N., Jin, Y., Hsu, A., Roukes, M. & Tian, L. "Letting the little light of mind shine: Advances and future directions in neurochemical detection". *Neurosci. Res.* **179**, 65–78 (2022).

138. Badgaiyan, R. D. Imaging dopamine neurotransmission in live human brain. *Prog. Brain Res.* **211**, 165–182 (2014).

139. Kilbourn, M. R. 11C- and 18F-Radiotracers for In Vivo Imaging of the Dopamine System: Past, Present and Future. *Biomedicines* **9**, 108 (2021).

140. Zürcher, N. R. *et al.* A simultaneous [11C]raclopride positron emission tomography and functional magnetic resonance imaging investigation of striatal dopamine binding in autism. *Transl. Psychiatry* **11**, 1–11 (2021).

141. Vaquero, J. J. & Kinahan, P. Positron Emission Tomography: Current Challenges and Opportunities for Technological Advances in Clinical and Preclinical Imaging Systems. *Annu. Rev. Biomed. Eng.* **17**, 385–414 (2015).

142. Jones, T. & Rabiner, E. A. The development, past achievements, and future directions of brain PET. *J. Cereb. Blood Flow Metab.* **32**, 1426–1454 (2012).

143. Cassidy, C. M. *et al.* Neuromelanin-sensitive MRI as a noninvasive proxy measure of dopamine function in the human brain. *Proc. Natl. Acad. Sci.* **116**, 5108–5117 (2019).

144. Berry, A. S. *et al.* Dopamine Synthesis Capacity is Associated with D2/3 Receptor Binding but Not Dopamine Release. *Neuropsychopharmacology* **43**, 1201–1211 (2018).

145. Jauhar, S. *et al.* Regulation of dopaminergic function: an [18F]-DOPA PET apomorphine challenge study in humans. *Transl. Psychiatry* **7**, e1027 (2017).

146. Cramb, K. M. L., Beccano-Kelly, D., Cragg, S. J. & Wade-Martins, R. Impaired dopamine release in Parkinson's disease. *Brain* **146**, 3117–3132 (2023).

147. Bhattacharjee, S., Shankar, P. V. & Elkider, M. Dopamine transporter single-photon emission computed tomography brain scan: A reliable way to distinguish between degenerative and drug-induced parkinsonism. *Indian J. Nucl. Med. IJNM Off. J. Soc. Nucl. Med. India* **31**, 249–250 (2016).

148. Lindon, J. C. SPECT, Methods and Instrumentation*. in *Encyclopedia of Spectroscopy and Spectrometry (Second Edition)* (ed. Lindon, J. C.) 2618–2619 (Academic Press, Oxford, 2010). doi:10.1016/B978-0-12-374413-5.00369-9.

149. Madsen, M. T. Recent Advances in SPECT Imaging. *J. Nucl. Med.* **48**, 661–673 (2007).

150. Brower, C. & Rehani, M. M. Radiation risk issues in recurrent imaging. *Br. J. Radiol.* **94**, 20210389 (2021).

151. Schulz, J., Zimmermann, J., Sorg, C., Menegaux, A. & Brandl, F. Magnetic resonance imaging of the dopamine system in schizophrenia – A scoping review. *Front. Psychiatry* **13**, 925476 (2022).

152. The physics of functional magnetic resonance imaging (fMRI) - PMC. https://www.ncbi.nlm.nih.gov/pmc/articles/PMC4376284/.

153. Mandeville, Joseph. B. *et al.* A receptor-based model for dopamine-induced fMRI signal. *NeuroImage* **75**, 46–57 (2013).

154. Wang, K. S., Smith, D. V. & Delgado, M. R. Using fMRI to study reward processing in humans: past, present, and future. *J. Neurophysiol.* **115**, 1664–1678 (2016).

155. Sander, C. Y., Hansen, H. D. & Wey, H.-Y. Advances in simultaneous PET/MR for imaging neuroreceptor function. *J. Cereb. Blood Flow Metab.* **40**, 1148–1166 (2020).

156. Al Haddad, R. *et al.* Normative Values of Neuromelanin-Sensitive MRI Signal in Older Adults Obtained Using a Turbo Spin Echo Sequence. *J. Magn. Reson. Imaging* **n/a**,.

157. Zucca, F. A. *et al.* Neuromelanins in brain aging and Parkinson's disease: synthesis, structure, neuroinflammatory, and neurodegenerative role. *Iubmb Life* **75**, 55–65 (2023).

158. Sulzer, D. *et al.* Neuromelanin detection by magnetic resonance imaging (MRI) and its promise as a biomarker for Parkinson's disease. *NPJ Park. Dis.* **4**, 11 (2018).

159. Zhou, Z. D., Yi, L. X., Wang, D. Q., Lim, T. M. & Tan, E. K. Role of dopamine in the pathophysiology of Parkinson's disease. *Transl. Neurodegener.* **12**, 44 (2023).

160. Moreno-García, A., Kun, A., Calero, M. & Calero, O. The Neuromelanin Paradox and Its Dual Role in Oxidative Stress and Neurodegeneration. *Antioxidants* **10**, 124 (2021).

161. Zecca, L., Tampellini, D., Rizzio, E., Giaveri, G. & Gallorini, M. The determination of iron and other metals by INAA in Cortex, Cerebellum and Putamen of human brain and in their neuromelanins. *J. Radioanal. Nucl. Chem.* **248**, 129–131 (2001).

162. Nash, K. M. & Ahmed, S. Nanomedicine in the ROS-Mediated Pathophysiology: Applications and Clinical Advances. *Nanomedicine Nanotechnol. Biol. Med.* **11**, 2033–2040 (2015).

163. Cassidy, C. *et al.* Neuromelanin-Sensitive MRI as an Index of Norepinephrine System Integrity in Healthy Aging, Mild Cognitive Impairment, and Alzheimer's Disease. *Biol. Psychiatry* **87**, S424–S425 (2020).

164. Qin, J., Ma, Z., Chen, X. & Shu, S. Microglia activation in central nervous system disorders: A review of recent mechanistic investigations and development efforts. *Front. Neurol.* **14**, 1103416 (2023).

165. Berger, A. Magnetic resonance imaging. *BMJ* **324**, 35 (2002).

166. Ryman, S. G. & Poston, K. L. MRI biomarkers of motor and non-motor symptoms in Parkinson's disease. *Parkinsonism Relat. Disord.* **73**, 85–93 (2020).

167. Chou, E. T. & Carrino, J. A. chapter 10 - Magnetic Resonance Imaging. in *Pain Management* (eds. Waldman, S. D. & Bloch, J. I.) 106–117 (W.B. Saunders, Philadelphia, 2007). doi:10.1016/B978-0-7216-0334-6.50014-5.

168. Pai, A., Shetty, R., Hodis, B. & Chowdhury, Y. S. Magnetic Resonance Imaging Physics. in *StatPearls* (StatPearls Publishing, Treasure Island (FL), 2024).

169. O'Reilly, T. & Webb, A. G. In vivo T1 and T2 relaxation time maps of brain tissue, skeletal muscle, and lipid measured in healthy volunteers at 50 mT. *Magn. Reson. Med.* **87**, 884–895 (2022).

170. Trujillo, P. *et al.* Quantitative magnetization transfer imaging of the human locus coeruleus. *NeuroImage* **200**, 191–198 (2019).

171. Dortch, R. D., Bagnato, F., Gochberg, D. F., Gore, J. C. & Smith, S. A. Optimization of Selective Inversion Recovery Magnetization Transfer Imaging for Macromolecular Content Mapping in the Human Brain. *Magn. Reson. Med.* **80**, 1824–1835 (2018).

172. van Zijl, P. C. M., Lam, W. W., Xu, J., Knutsson, L. & Stanisz, G. J. Magnetization Transfer Contrast and Chemical Exchange Saturation Transfer MRI. Features and Analysis of the Field-Dependent Saturation Spectrum. *NeuroImage* **168**, 222–241 (2018).

173. Magnetization Transfer Imaging. *Questions and Answers in MRI* http://mriquestions.com/mt-imagingcontrast.html.

174. Structure-Relaxivity Relationships of Magnetic Nanoparticles for Magnetic Resonance Imaging - PMC. https://www.ncbi.nlm.nih.gov/pmc/articles/PMC6392011/.

175. Chavhan, G. B., Babyn, P. S., Thomas, B., Shroff, M. M. & Haacke, E. M. Principles, Techniques, and Applications of T2*-based MR Imaging and Its Special Applications. *RadioGraphics* **29**, 1433–1449 (2009).

176. Poustchi-Amin, M., Mirowitz, S. A., Brown, J. J., McKinstry, R. C. & Li, T. Principles and applications of echo-planar imaging: a review for the general radiologist. *Radiogr. Rev. Publ. Radiol. Soc. N. Am. Inc* **21**, 767–779 (2001).

177. Thomas, D. L. *et al.* High-Resolution Fast Spin Echo Imaging of the Human Brain at 4.7 T: Implementation and Sequence Characteristics. *Magn. Reson. Med. Off. J. Soc. Magn. Reson. Med. Soc. Magn. Reson. Med.* **51**, 1254–1264 (2004).

178. Mullen, M. & Garwood, M. Contemporary approaches to high-field magnetic resonance imaging with large field inhomogeneity. *Prog. Nucl. Magn. Reson. Spectrosc.* **120–121**, 95–108 (2020).

179. Tripp, G. & Wickens, J. Using rodent data to elucidate dopaminergic mechanisms of ADHD: Implications for human personality. *Personal. Neurosci.* **7**, e2 (2024).

180. Ernst, M. *et al.* High midbrain [18F]DOPA accumulation in children with attention deficit hyperactivity disorder. *Am. J. Psychiatry* **156**, 1209–1215 (1999).

181. Lau, J. *et al.* Insight into the Development of PET Radiopharmaceuticals for Oncology. *Cancers* **12**, 1312 (2020).

182. Synowiecki, M. A., Perk, L. R. & Nijsen, J. F. W. Production of novel diagnostic radionuclides in small medical cyclotrons. *EJNMMI Radiopharm. Chem.* **3**, 3 (2018).

183. Zecca, L. *et al.* The absolute concentration of nigral neuromelanin, assayed by a new sensitive method, increases throughout the life and is dramatically decreased in Parkinson's disease. *FEBS Lett.* **510**, 216–220 (2002).

184. Huddleston, D. E. *et al.* Neuromelanin-sensitive MRI correlates of cognitive and motor function in Parkinson's disease with freezing of gait. *medRxiv* 2023.07.04.23292227 (2023) doi:10.1101/2023.07.04.23292227.

185. Konnova, E. A. & Swanberg, M. Animal Models of Parkinson's Disease. in *Parkinson's Disease: Pathogenesis and Clinical Aspects* (eds. Stoker, T. B. & Greenland, J. C.) (Codon Publications, Brisbane (AU), 2018).

186. Ciampa, C. J. *et al.* Elevated Dopamine Synthesis as a Mechanism of Cognitive Resilience in Aging. *Cereb. Cortex N. Y. NY* **32**, 2762–2772 (2021).

187. LUCIANA, M. Adolescent brain development in normality and psychopathology. *Dev. Psychopathol.* **25**, 1325–1345 (2013).

188. Kollins, S. H. & Adcock, R. A. ADHD, Altered Dopamine Neurotransmission, and Disrupted Reinforcement Processes: Implications for Smoking and Nicotine Dependence. *Prog. Neuropsychopharmacol. Biol. Psychiatry* **0**, 70–78 (2014).

189. Hesse, S., Ballaschke, O., Barthel, H. & Sabri, O. Dopamine transporter imaging in adult patients with attention-deficit/hyperactivity disorder. *Psychiatry Res.* **171**, 120–128 (2009).

190. da Silva, B. S. *et al.* An overview on neurobiology and therapeutics of attention-deficit/hyperactivity disorder. *Discov. Ment. Health* **3**, 2 (2023).

191. Faraone, S. V. The Pharmacology of Amphetamine and Methylphenidate: Relevance to the Neurobiology of Attention-Deficit/Hyperactivity Disorder and Other Psychiatric Comorbidities. *Neurosci. Biobehav. Rev.* **87**, 255–270 (2018).

192. Mechler, K., Banaschewski, T., Hohmann, S. & Häge, A. Evidence-based pharmacological treatment options for ADHD in children and adolescents. *Pharmacol. Ther.* **230**, 107940 (2022).

193. Nazarova, V. A., Sokolov, A. V., Chubarev, V. N., Tarasov, V. V. & Schiöth, H. B. Treatment of ADHD: Drugs, psychological therapies, devices, complementary and alternative methods as well as the trends in clinical trials. *Front. Pharmacol.* **13**, 1066988 (2022).

194. Matthys, W. & Schutter, D. J. L. G. Increasing Effectiveness of Cognitive Behavioral Therapy for Conduct Problems in Children and Adolescents: What Can We Learn from Neuroimaging Studies? *Clin. Child Fam. Psychol. Rev.* **24**, 484–499 (2021).

195. Holton, K. F. & Nigg, J. T. The Association of Lifestyle Factors and ADHD in Children. *J. Atten. Disord.* **24**, 1511–1520 (2020).

196. Pickersgill, J. W. *et al.* The Combined Influences of Exercise, Diet and Sleep on Neuroplasticity. *Front. Psychol.* **13**, 831819 (2022).

197. Staff, A. I., Oosterlaan, J., van der Oord, S., van den Hoofdakker, B. J. & Luman, M. The Relation Between Classroom Setting and ADHD Behavior in Children With ADHD Compared to Typically Developing Peers. *J. Atten. Disord.* **27**, 939–950 (2023).

198. van der Pluijm, M. *et al.* Reliability and Reproducibility of Neuromelanin-Sensitive Imaging of the Substantia Nigra: A Comparison of Three Different Sequences. *J. Magn. Reson. Imaging* **53**, 712–721 (2021).

199. Wengler, K., He, X., Abi-Dargham, A. & Horga, G. Reproducibility assessment of neuromelanin-sensitive magnetic resonance imaging protocols for region-of-interest and voxelwise analyses. *NeuroImage* **208**, 116457 (2020).

200. Tulsky, D. S. *et al.* NIH Toolbox Cognition Battery (NIHTB-CB): list sorting test to measure working memory. *J. Int. Neuropsychol. Soc. JINS* **20**, 599–610 (2014).

201. Zelazo, P. D. *et al.* NIH Toolbox Cognition Battery (CB): Validation of Executive Function Measures in Adults. *J. Int. Neuropsychol. Soc. JINS* **20**, 620–629 (2014).

202. Wengler, K. *et al.* Cross-Scanner Harmonization of Neuromelanin-Sensitive MRI for Multisite Studies. *J. Magn. Reson. Imaging JMRI* **54**, 1189–1199 (2021).

203. Riley, E., Cicero, N., Swallow, K., De Rosa, E. & Anderson, A. Locus coeruleus neuromelanin accumulation and dissipation across the lifespan. *bioRxiv* 2023.10.17.562814 (2023) doi:10.1101/2023.10.17.562814.

204. Mattson, M. P. & Magnus, T. Aging and Neuronal Vulnerability. *Nat. Rev. Neurosci.* **7**, 278–294 (2006).

205. Nguyen, L., Murphy, K. & Andrews, G. Cognitive and neural plasticity in old age: A systematic review of evidence from executive functions cognitive training. *Ageing Res. Rev.* **53**, 100912 (2019).

206. Wise, R. M. *et al.* Interactions of dopamine, iron, and alpha-synuclein linked to dopaminergic neuron vulnerability in Parkinson's disease and Neurodegeneration with Brain Iron Accumulation disorders. *Neurobiol. Dis.* **175**, 105920 (2022).

207. Trist, B. G., Hare, D. J. & Double, K. L. Oxidative stress in the aging substantia nigra and the etiology of Parkinson's disease. *Aging Cell* **18**, e13031 (2019).

208. Berkowitz, S. J. *et al.* Axial Black Blood Turbo Spin Echo Imaging of the Right Ventricle. *Magn. Reson. Med. Off. J. Soc. Magn. Reson. Med. Soc. Magn. Reson. Med.* **61**, 307–314 (2009).

209. Martinez, D. *et al.* Dopamine type 2/3 receptor availability in the striatum and social status in human volunteers. *Biol. Psychiatry* **67**, 275–278 (2010).

210. Bush, G. Attention-Deficit/Hyperactivity Disorder and Attention Networks. *Neuropsychopharmacology* **35**, 278–300 (2010).

211. Zhang, R., Murray, S. B., Duval, C. J., Wang, D. J. J. & Jann, K. Functional connectivity and complexity analyses of resting-state fMRI in pre-adolescents demonstrating the behavioral symptoms of ADHD. *Psychiatry Res.* **334**, 115794 (2024).

212. Krause, J. SPECT and PET of the dopamine transporter in attention-deficit/hyperactivity disorder. *Expert Rev. Neurother.* **8**, 611–625 (2008).

213. Schreiber, J. E., Possin, K. L., Girard, J. M. & Rey-Casserly, C. Executive Function in Children with Attention Deficit/Hyperactivity Disorder: the NIH EXAMINER battery. *J. Int. Neuropsychol. Soc. JINS* **20**, 41–51 (2014).

214. Barber, A. D. *et al.* Motor "Dexterity"?: Evidence that Left Hemisphere Lateralization of Motor Circuit Connectivity Is Associated with Better Motor Performance in Children. *Cereb. Cortex N. Y. NY* **22**, 51–59 (2012).

215. Martínez, M. *et al.* Brainstem neuromelanin and iron MRI reveals a precise signature for idiopathic and LRRK2 Parkinson's disease. *Npj Park. Dis.* **9**, 1–11 (2023).